

## General Disclaimer

### One or more of the Following Statements may affect this Document

- This document has been reproduced from the best copy furnished by the organizational source. It is being released in the interest of making available as much information as possible.
- This document may contain data, which exceeds the sheet parameters. It was furnished in this condition by the organizational source and is the best copy available.
- This document may contain tone-on-tone or color graphs, charts and/or pictures, which have been reproduced in black and white.
- This document is paginated as submitted by the original source.
- Portions of this document are not fully legible due to the historical nature of some of the material. However, it is the best reproduction available from the original submission.

LOW COST SOLAR ARRAY PROJECT  
Production Process and Equipment Task

A MODULE EXPERIMENTAL PROCESS SYSTEM DEVELOPMENT UNIT (MEPSDU)

SUMMARY TECHNICAL REPORT

November 26, 1980 to February 10, 1982

Contract No. 955909

The JPL Low-Cost Silicon Array Project is sponsored by the U. S. Department of Energy and forms part of the Solar Photovoltaic Conversion Program to initiate a major effort toward the development of low-cost solar arrays. This work was performed for the Jet Propulsion Laboratory, California Institute of Technology, by agreement between NASA and DOE.

Approved:



---

C. M. Rose, Project Manager  
Photovoltaic Components

Advanced Energy Systems Division  
WESTINGHOUSE ELECTRIC CORPORATION  
P. O. Box 10864  
Pittsburgh, Pennsylvania 15236

### TECHNICAL CONTENT STATEMENT

"This report was prepared as an account of work sponsored by the United States Government. Neither the United States nor the United States Department of Energy, nor any of their employees, nor any of their contractors, subcontractors, or their employees, makes any warranty, express or implied, or assumes any legal liability or responsibility for the accuracy, completeness or usefulness of any information, apparatus, product or process disclosed, or represents that its use would not infringe privately owned rights."

## TABLE OF CONTENTS

	Page
I. CONTRACT GOALS AND OBJECTIVES. . . . .	1
II. SUMMARY. . . . .	2
III. SELECTION OF INPUT SHEET MATERIAL. . . . .	5
IV. MEPSDU Module. . . . .	11
A. Module Design. . . . .	11
1. Mechanical . . . . .	11
2. Interface. . . . .	14
3. Electrical Design. . . . .	16
B. Module Performance Evaluation. . . . .	24
C. Environmental Testing. . . . .	31
1. Hailstone Impact Tests . . . . .	31
2. Wind Load Testing. . . . .	31
3. Thermal and Humidity Cyclic Tests. . . . .	32
4. Loss of Cell Contact Pad Electrical Connection . . . . .	41
5. Cell Shading Tests . . . . .	44
V. PROCESS SEQUENCE DESIGN. . . . .	48
A. Baseline Process Sequence. . . . .	48
B. Alternate Process Sequence Steps . . . . .	55
1. Alternate Metallization Procedures . . . . .	55
2. Dry Processing Experiments . . . . .	57
3. Liquid Precursor Films for Diffusion Masks . . . . .	61
4. Liquid Dopant Diffusant Studies. . . . .	62
VI. MEPSDU Design. . . . .	67
A. General. . . . .	67
B. Pre-Diffusion Cleaning . . . . .	67
C. Junction Formation Station . . . . .	68
D. Antireflective (AR) and Photoresist (PR) Application Stations. . . . .	69
E. Expose/Develop/Etch Station. . . . .	71
F. Metallization Box Coater . . . . .	72
G. Metal Rejection/Plating Station. . . . .	74
H. Cell Separation Station. . . . .	76
I. Cell/Module Test Stations. . . . .	80



TABLE OF CONTENTS (Continued)

	Page
VII. KULICKE AND SOFFA SUBCONTRACT . . . . .	82
A. General . . . . .	82
B. Bonder . . . . .	84
C. Cassette Unload Station . . . . .	89
D. Bond Stations . . . . .	89
E. String Conveyor . . . . .	92
F. Control System . . . . .	93
G. Design Review . . . . .	94
VIII. ECONOMIC ANALYSES . . . . .	96
A. Background . . . . .	96
B. Assumptions Used in SAMICS Cost Analyses . . . . .	98
C. Results and Conclusions . . . . .	99
IX. DOCUMENTATION . . . . .	104

## LIST OF TABLES

	Page
1. A Comparison of Candidate Sheet Forms for MEPSDU. . . . .	6
2. Specification for Polycrystalline Silicon to be Used in Westinghouse MEPSDU Sheet Material . . . . .	10
3. MEPSDU Dendritic Web Input Sheet Material Specification (Preliminary). . . . .	11
4. Major Westinghouse MEPSDU Module Design Innovations . . . . .	13
5. Calculated MEPSDU Module Performance Parameters . . . . .	29
6. Layup of Small Modules Used for Environmental Testing . . . . .	33
7. Pre- and Post-Lamination Measurements of Cell String Characteristics. . . . .	37
8. Measurements Made on Thermally Cycled Test Modules. . . . .	39
9. Measurements Made on Environmental Test Modules . . . . .	40
10. Output Power from Solar Cell as Function of Interconnect Pads Contacted . . . . .	43
11. Plasma Etching of Raw Web . . . . .	60
12. Comparison of Cells Produced Using the Baseline Process (Gaseous Diffusion) and Liquid Dopants . . . . .	64
13. Metallization Box Coater Specification Highlights . . . . .	73
14. Rejection/Plating Station Treatment Cycle . . . . .	75
15. Novel Features of the Westinghouse MEPSDU Facility Laser Scribe . .	78
16. MEPSDU Laser Scribe Automatic Alignment System Features . . . . .	79
17. Laser Scribe Time Budgets . . . . .	81
18. Processes and Referents Used in SAMICS Cost Analyses. . . . .	97
19. SAMICS Cost Analysis (1MW/yr Production Facility) . . . . .	100
20. SAMICS Cost Analysis (25 MW/yr Production Facility) . . . . .	102
21. SAMICS Cost Analysis. . . . .	103
22. MEPSDU Programmable Documentation Submittal Status. . . . .	105

## LIST OF FIGURES

	Page
1. Westinghouse Dendritic Web being Removed from the Dendritic Web Growth Furnace. . . . .	7
2. Westinghouse MEPSDU Module Assembly Drawing. . . . .	12
3. Prototype MEPSDU Module Fabricated in Westinghouse Pre-Pilot Facility. . . . .	15
4. Glass Panelled Wall Utilizing Structural Adhesive Supports . . . . .	17
5. Geometry of Ultrasonic Bonds, Dark Side. . . . .	19
6. Cell Interconnection Geometry. . . . .	21
7. Layup Materials and Dimensions of the Westinghouse MEPSDU Module . . . . .	26
8. Calculated MEPSDU Module $V_{oc}$ and $I_{sc}$ as Functions of Ambient Temperature . . . . .	27
9. Calculated MEPSDU Module Power and Efficiency as Functions of Ambient Temperature . . . . .	28
10. I-V Test Curve of Prototype MEPSDU Module. . . . .	30
11. Environmental Test Module G-2 (10 cm x 9 cm) . . . . .	35
12. Environmental Test Modules in Humidity Test Fixture. . . . .	36
13. Environmental Test Data from Minimodule G-2. . . . .	42
14. Test System Used for Cell Shading Tests. . . . .	45
15. Shadowed Cell Heating Effects under Module Short Circuit Conditions. . . . .	46
16. Westinghouse MEPSDU Overall Process Sequence . . . . .	49
17. Westinghouse MEPSDU Baseline Process Sequence Flow Chart . . . . .	50
18. Westinghouse MEPSDU Module Assembly Flow Chart . . . . .	53
19. Meniscus Coating of Precursor Fluids to Dendritic Web Silicon. . . . .	66
20. Automated Laser Scribe . . . . .	77
21. Westinghouse MEPSDU Automated Cell Interconnect Station. . . . .	83
22. Rotary Ultrasonic Seam Bonding . . . . .	85
23. Rolling Spot Ultrasonic Bonding. . . . .	86
24. Bonding Mechanism for First Bond Station . . . . .	88
25. Mockup of Cassette Unload Station. . . . .	90
26. Interconnect Feed Station (Minus Ribbon Transfer Mechanism). . . . .	91
27. Interconnect Station Control Structure . . . . .	95

## I. CONTRACT GOALS AND OBJECTIVES

The objective of this contract, as it was originally written, was to determine technical feasibility of the production of photovoltaic modules designed to meet all environmental specifications described in JPL Document 510i-138, fabricated using single crystal silicon dendritic web sheet material, and meeting JPL's 1986 production cost goals of 70¢/peak watt (1980\$). This determination of technical feasibility was to be accomplished by:

- A. The design of a flat plate photovoltaic module utilizing dendritic web sheet material and meeting all environmental specifications contained in JPL Document 510i-138,
- B. The selection, design, and implementation of a solar cell processing and photovoltaic assembly sequence for fabricating modules of the specified design (Item A above) in a Module Experimental Process System Development Unit (MEPSDU),
- C. Performance of technical feasibility experiments in which a sufficient number of modules were to be produced in the MEPSDU facility to allow assessment of production costs,
- D. Passing of acceptance and qualification tests by modules produced during the demonstration runs, and
- E. Projection of a 1986 module FOB mass production cost in a fully automated, 25 MW/yr capacity facility using the MEPSDU process sequence as calculated by SAMICS using cost data generated during completion of the demonstration runs (Item C above).

**ORIGINAL PAGE IS  
OF POOR QUALITY**

II. SUMMARY

Work on the Westinghouse MEPSDU contract was initiated on November 26, 1980. This report summarizes all technical progress made on the contract from the initiation date until a stop work order was received from JPL on February 10, 1982. In the stop work order, the contract was restructured from a technical readiness demonstration program to an investigation of high-risk, high-payoff research areas associated with the Westinghouse process for producing photovoltaic modules using non-CZ sheet material. It was emphasized in the JPL stop work order that the "restructuring in no way reflects adversely upon the contracted performance of Westinghouse, but is intended to comply with the Department of Energy guidelines for funding high-risk, high-payoff research projects."

Prior to the stop work order, two contract modifications had been effected by JPL which reduced program expenditure rates from those of the original contract. However, in all cases the contract goals and objectives as presented in Section I of this report remained unchanged.

The first major program milestone, Preliminary Design Review (PDR), was met as scheduled with a formal presentation at JPL on March 4 and 5, 1981. This was preceded by the submittal of the Preliminary Design Review Data Package consisting of:

- A Preliminary Specification for MEPSDU Input Sheet Material (Dendritic Web Silicon),
- A MEPSDU Module Preliminary Design Layout Drawing and all associated detail drawings,
- Analysis of the performance of the MEPSDU module over a range of operating conditions,
- Definition of all steps in the Baseline Process Sequence,

- Equipment Specifications for all long-lead time items in the MEPSDU,
- Preliminary design of the cassette unload element and interconnect feed elements of the automated cell interconnect station, and
- The Preliminary Quality Assurance Plan.

The second major program milestone, Final MEPSDU Module Design Review (MDR), was a formal presentation at JPL on July 14, 1981. This was preceded by the Design Review Data Package submittal consisting of:

- Copies of viewgraph materials,
- All module drawings,
- The module materials selection sheet,
- Performance predictions, and
- Module manufacturing flow information.

The module design matured substantially between the PDR and the MDR. Many of the improvements stemmed from comments received from JPL personnel at the PDR. The most significant improvement was the deletion of the module frame in favor of a "frameless" design which provides a substantially improved cell packing factor, hence overall efficiency. Also, a modification was made in the cell series/parallel electrical interconnect configuration to eliminate potential shaded cell damage resulting from operation into a short circuit.

Through work on this contract, a Baseline Process Sequence was identified for the fabrication of modules using the selected dendritic web sheet material. This baseline process was incorporated in the Westinghouse Pre-Pilot Photovoltaic Module Production Facility. Although this facility is a non-automated, limited volume facility, prototype modules of the MEPSDU design were fabricated using the baseline process sequence. (The assembly work was completed as part of a non-Government funded project.) Subsequently, extensive tests on full-size and mini-size prototype modules verified compliance of the basic layout configuration with environmental specifications of JPL Document 5101-138. In addition,

performance data from prototype modules fabricated using the baseline process sequence demonstrated that an overall module efficiency level of 12% projected at the beginning of the contract was achieved.

Economic evaluations of the Westinghouse Baseline Process Sequence have been completed, using formal Solar Array Manufacturing Industry Costing Standards (SAMICS) techniques. These evaluations were performed in close coordination with JPL personnel who completed similar but parallel economic analyses of the Westinghouse MEPSDU process sequence. Results of these analyses have verified that the process sequence defined in this program for manufacturing photovoltaic modules from dendritic web silicon can meet the JPL long range cost objectives of 70¢/peak watt (1980\$) in a fully automated production facility.

When the Westinghouse MEPSDU contract stop work order was received from JPL, all technical and documentation tasks were on the schedule defined in the contract program plan. Referring to the contract goals and objectives listed in Section I of this report, Item A (module design) was complete; and Item B (MEPSDU facility design) was essentially complete.

The baseline process sequence had been established and verified, and nearly all equipment required for a 1 MW/yr demonstration facility had been formally specified. Some long lead equipment (i.e., laser scribe, semi-automated cell and module test equipment, and automated cell interconnect station) had been placed on order.

Based on the success of this program, Westinghouse Electric Corporation, which had previously committed to procure the capital equipment required for the 1 MW/yr demonstration facility, has decided to complete the design, procurement, and installation tasks with corporate funding. JPL funding will continue for two highly developmental, but promising, research and development tasks that could result in substantial improvement in the cost effectiveness of the baseline process sequence.

MEPSDU project costs were consistent with budget projections at the time of the stop work order issuance. The remaining research tasks are being completed on a significantly reduced budget level.

### III. SELECTION OF INPUT SHEET MATERIAL

The first technical milestone of the MEPSDU contract was the selection of input sheet material to be used for the manufacture of solar cells produced in the MEPSDU facility.

A study of the significant parameters of all candidate sheet forms was made, and Table 1 summarizes the results of this analysis. As is shown in Table 1, each of the sheet input forms has favorable characteristics. However, the Westinghouse dendritic web excels in nearly every category and is the clear-cut front runner in providing the high efficiency, high reliability, and low cost demanded by the low cost solar array program objectives. Thus, single crystal dendritic web silicon was selected as the Westinghouse MEPSDU input sheet material.

Figure 1 shows a length of dendritic web silicon in the as-grown condition being removed from a growth furnace at the Westinghouse pre-pilot facility. The shape of the dendritic web is determined by a combination of crystallographic and surface tension forces as it is formed from the molten silicon. The absence of any die material precludes contamination and die material inclusions which are known problems with other ribbon growth techniques. Cells fabricated on dendritic web have shown efficiencies comparable to cells fabricated on Czochralski wafers (15 to 17%). The process conserves expensive silicon since the as-grown material is thin - 110 to 170  $\mu\text{m}$  - and the smooth surface does not require extensive treatment prior to cell fabrication.

The natural rectangular shape of cells fabricated on dendritic web permits high module packing factors which contributes to high module efficiency.

Investigations in the production and application of photovoltaic modules have confirmed that high module efficiency has many benefits ranging from decreased module encapsulation costs to significant balance of system and installation cost savings. In the area of module fabrication alone, a cost saving of six cents per watt is associated with each 1% increase in module efficiency. High quality starting material is essential to producing high efficiency cells and



ORIGINAL PAGE IS  
OF POOR QUALITY

TABLE 1  
A COMPARISON OF CANDIDATE SHEET FORMS FOR MEPSDU

Parameter	Westinghouse Dendritic Web	EFG	CZ	HEM	SEMIX
Demonstrated Cell Efficiency	High	Medium	High	Medium	Medium
Module Efficiency	12-16%	7-10%	8-16%	8-11%	7-10%
Cell Interconnection Redundancy	High	High	Low	Medium	High
Growth Rate	Medium	High	Medium	High	High
Crystal Quality	Single	Poly	Single	Poly	Poly
Module Packing Fraction	High	High	Low	Medium	High
Silicon Utilization	3 kg/kw	8 kg/kw	12 kg/kw	12 kg/kw	8 kg/kw
Slicing Requirement	No	No	Yes	Yes	Yes
SAMICS Cost Catalog	\$30/m <sup>2</sup>	\$27/m <sup>2</sup>	\$47/m <sup>2</sup>	\$40/m <sup>2</sup>	

EFG - Edge Defined Film Fed Growth (Mobil Tyco)

Cz - Czochralski Wafers

HEM - Heat Exchanger Method (Crystal Systems)

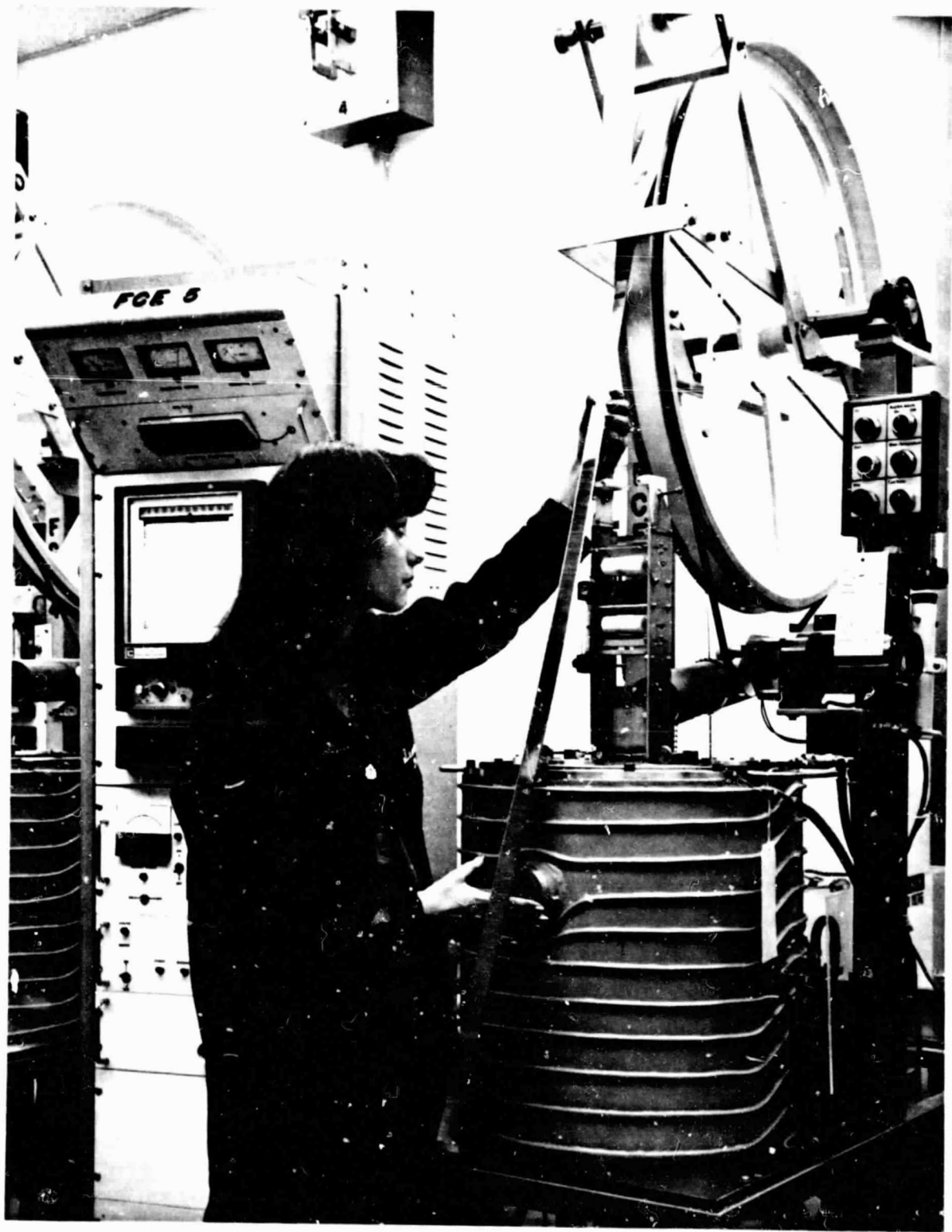


Figure 1. Westinghouse Dendritic Web being Removed from the Dendritic Web Growth Furnace

modules. Dendritic web is high quality, single crystal silicon, and has already been used in fabricating photovoltaic cells with efficiencies greater than 15% and modules with efficiencies greater than 12%.

A preliminary material specification for the polycrystalline silicon used as a feed stock in the dendritic web furnaces has been prepared and is shown in Table 2. Table 3 shows the preliminary material specification for the dendritic web silicon sheet input.

**TABLE 2**

**SPECIFICATION FOR POLYCRYSTALLINE SILICON TO BE USED  
IN WESTINGHOUSE MEPSDU SHEET MATERIAL**

- Boule to be 5-10 cm in diameter
- Random lengths acceptable, but length must be in excess of 15 cm
- Less than 0.3 PPBA (parts per billion atoms) boron concentration
- Less than 0.5 PPBA phosphorous concentration
- Less than 10 PPBA aluminum concentration
- Total of all other metals less than 5 PPBA concentration

TABLE 3

MEPSDU DENDRITIC WEB INPUT SHEET MATERIAL SPECIFICATION  
(PRELIMINARY)

I. Chemical

- A. Single crystal silicon with [111] web surface orientation
- B. P-type material with boron based dopant providing a resistivity in the range 3 to 12 ohm cm

II. Physical

- A. Thickness of web:  $140 \pm 30 \mu\text{m}$
- B. Width of web: Equal to or greater than 2.55 cm excluding dendrites
- C. Length\* of web:  $43 \pm .5 \text{ cm}$
- D. Surface striations across web not to exceed  $1 \mu\text{m}$  height as measured by a thickness monitor such as "Taly-Step" or "Data-Trak"
- E. Etch pit density (determined after 5 min. Sirtl etch) not to exceed  $3 \times 10^4/\text{cm}^2$
- F. Flatness: No twist or bow as determined by visual inspection

---

\*Shorter lengths are acceptable but will produce less than 4 cells/strip, thus reducing yield of all cell processing operations.

#### IV. MEPSDU MODULE

##### A. Module Design

###### 1. Mechanical

The second technical milestone of the MEPSDU contract was the design of a flat plate photovoltaic module meeting all environmental specifications contained in JPL Document 5101-138.

The MEPSDU Preliminary Design Review was held at JPL on March 4 and 5, 1981. A preliminary module design was presented at that time. The Prototype Module Design Review was conducted at JPL on July 14, 1981. In general, the design was well received. Some concern was expressed by JPL personnel for the unprotected edges of the tempered glass superstrate in the Westinghouse frameless module design. Resolution of this concern was deferred pending completion of hail impact tests which were conducted after the design review and which confirmed that the glass could withstand corner impacts without damage. These and other environmental tests are discussed below.

The assembly drawing of the prototype Westinghouse MEPSDU module (Westinghouse Drawing 712J927) is shown in Figure 2. The most significant innovations included in the design are summarized in Table 4.

The MEPSDU module assembly drawing specifies a superstrate of 1/8 inch thick tempered glass with an iron content of less than 0.03%. With this low iron content, the solar transmittance in the 0.4 to 1.2  $\mu\text{m}$  wavelength range is 91%. This is a significant improvement over standard tempered glass which transmits less than 87%. The remaining loss in transmittance is mainly ( $\approx 80-90\%$ ) a reflection loss.

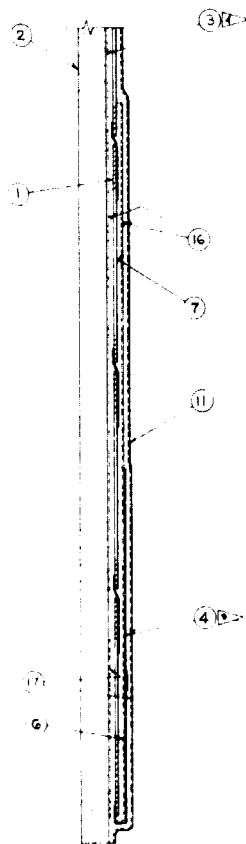
Working with a vendor after completion of the module assembly drawing, an even greater transmittance was achieved through a proprietary surface treatment. This treatment is based on work initiated on an ERDA program<sup>(1)</sup> and improved by later industry studies<sup>(2)</sup>. The treatment consists of etching the glass in

(1) Phase II Final Report, C00-2930-12 to ERDA from Honeywell Corporation.

(2) Zuel Corporation, St. Paul, Minnesota.

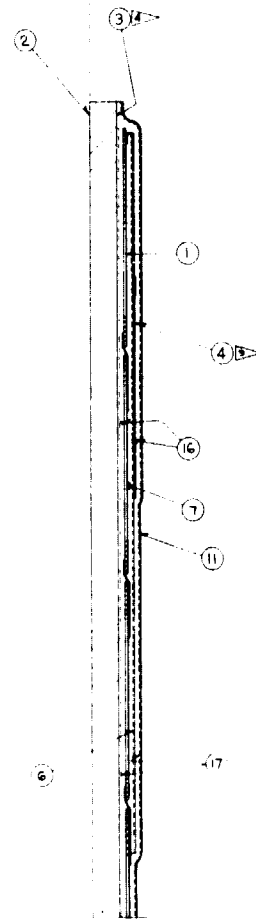
FOLDOUT FRAME

ORIGINAL PAGE IS  
OF POOR QUALITY

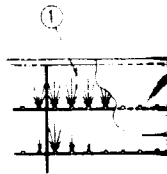


SECT D-D (r2)

FINE MATTE SURFACE OF  
IT 2 LOCATED THIS SIDE

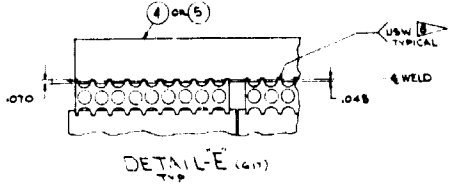


SECT C-C (r2)

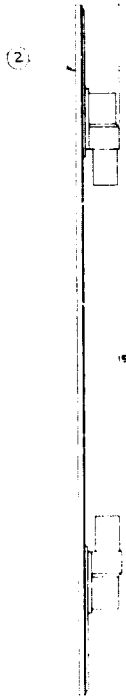
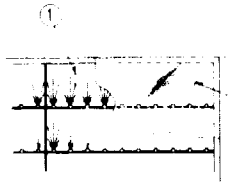


FOLDOUL FRAME 2

18 17 16 15 14 13

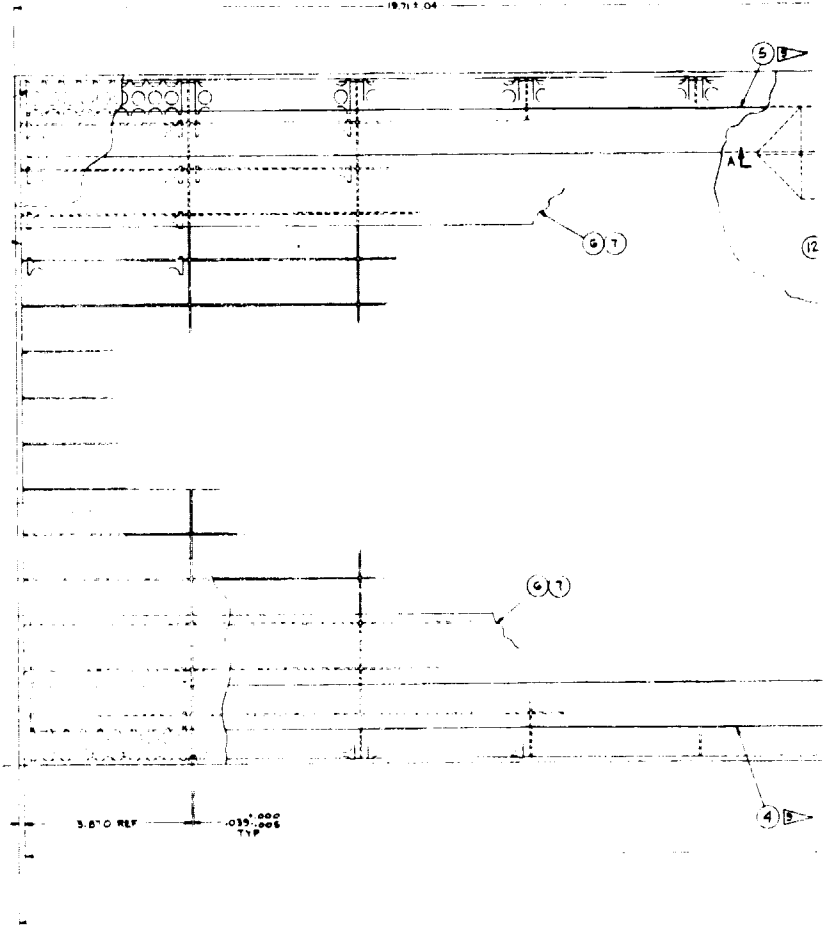


1.00 TIP



SEE DETAIL E (a) FOR WELDING PRIOR TO FOLD OVER AS SHOWN TYP

15.00 REF B



3.8" REF .035" .006 TIP

ORIGINAL PAGE IS OF POOR QUALITY

18 17 16 15 14 13



ORIGINAL PAGE IS  
OF POOR QUALITY

FOLDOUT FRAME

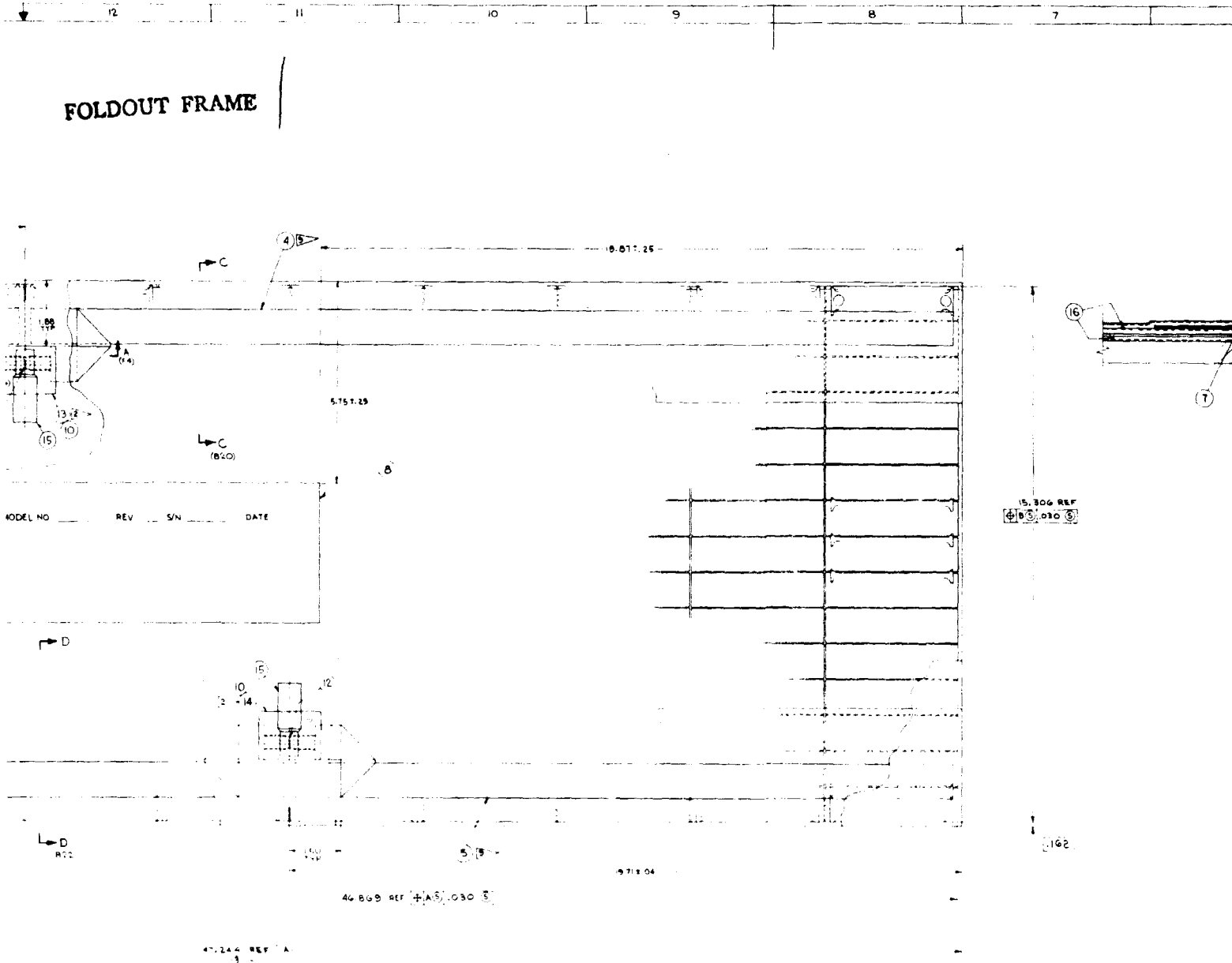


TABLE 1	
GROUP NO.	PART
1	2.9E



#### TABLE 4

##### MAJOR WESTINGHOUSE MEPSDU MODULE DESIGN INNOVATIONS

- Use of dendritic web single-crystal silicon
- Use of high aspect ratio (3.9:1) rectangular photovoltaic cells
- Tempered glass superstrate
- Antireflectance treated front glass surface
- Frameless construction
- Elimination of solder joints inside the encapsulation envelope
- High cell interconnect redundancy
- 12 parallel cell circuits

a controlled manner to produce micro-pores on the surface (10-30Å across) which act as an antireflective coating. The index of refraction of this surface matches the glass-air interface and reduces reflection losses.

Samples of this glass with this surface treatment have been on test at the Los Alamos Test Center for over 12 months, and no degradation in transmittance has been noted.

Several pieces of module sized glass (nominal 16" x 48"), prepared with the antireflective surface treatment, were procured for test purposes. The treated surfaces show a bluish tint as would be noted with a very thin antireflective coating. Tests indicate that this treated glass increases the transmittance from 91% to 96%. On a high efficiency module ( $\approx 12\%$ ), this increased transmittance translates into about 0.5% absolute increase in module efficiency.

Several laminations were carried out using this glass without difficulty. Subsequently, all modules fabricated on the Westinghouse pre-pilot facility have incorporated this glass treatment.

Figure 3 is a photograph of one of the first prototype MEPSDU modules fabricated in the Westinghouse Pre-Pilot Facility. Visible in the photograph is the 12 x 15 array of solar cells. Each cell is nominally 1 in. (2.5 cm) by 4 in. (9.83 cm), and the nominal module dimensions are 16 in. (39.7 cm) by 48 in. (119.9 cm). Nominal output power of the module is 55 watts (peak).

## 2. Interface

Perhaps the most significant innovation of the Westinghouse module is the elimination of a module frame. This design allows placement of photovoltaic cells under a much larger percentage of the superstrate surface than is possible when using a frame. The modules are to be attached to and supported from the array structure, test rack, or roof structure through a structural adhesive system. The adhesive system consists of two components: strips or patches of double-faced polyurethane adhesive tape and a silicone adhesive/sealant. The tape provides immediate low strength attachment and stand-off of the module to the

ORIGINAL PAGE  
BLACK AND WHITE PHOTOGRAPH

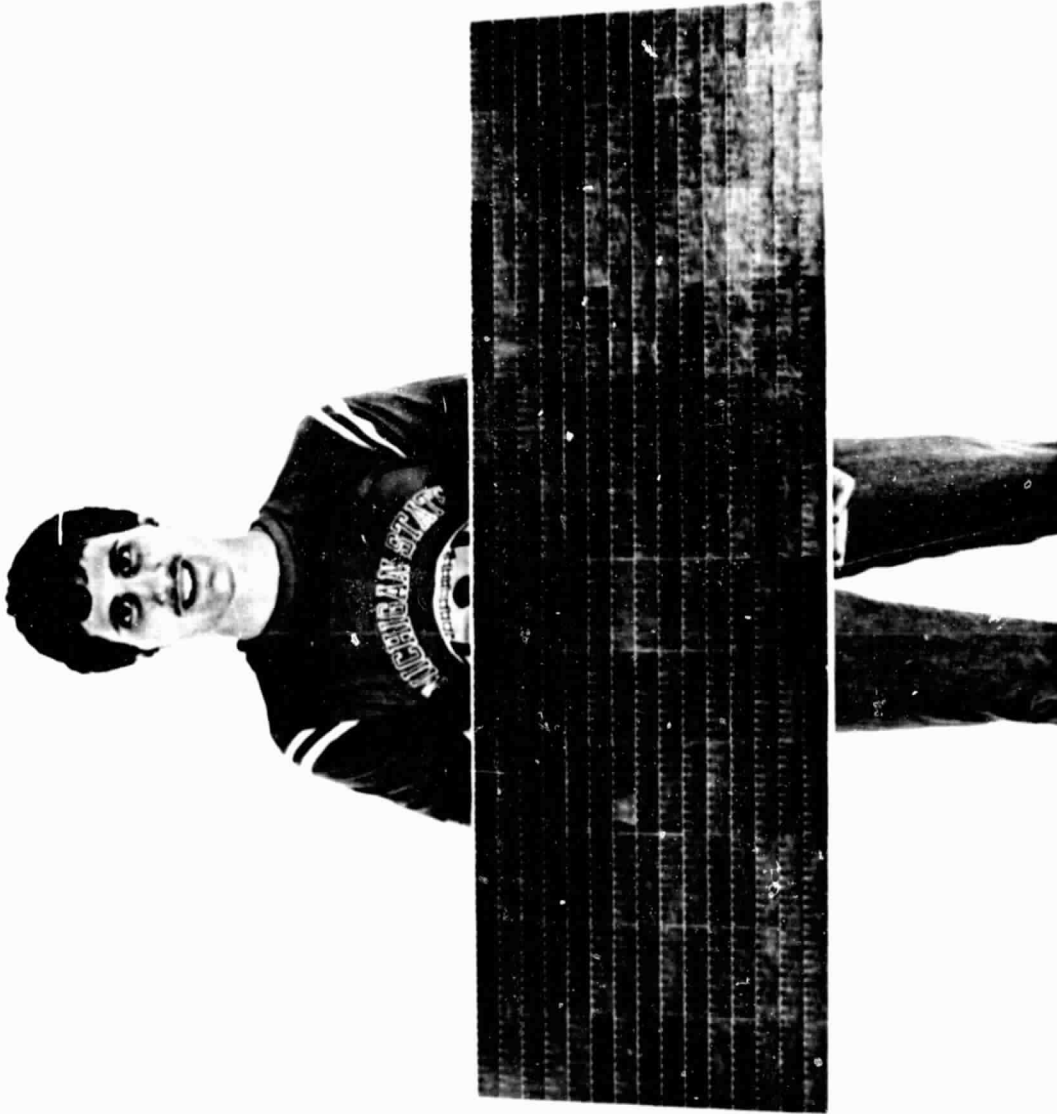


Figure 3. Prototype MEPSDU Module Fabricated  
in Westinghouse Pre-Pilot Facility

support structure. The adhesive/sealant fills the gaps between the support structure and module and provides a high strength intermediate modulus attachment when cured under ambient conditions. A significant feature of this support system is that application of the adhesive is a field operation rather than a shop operation. No silicones will be present in the shop environment prior to lamination, and the lamination operation is completed several days to several weeks before the module encounters the silicone adhesive.

Although this support system has never been used (to our knowledge) on photovoltaic module arrays, it has been used successfully in architectural applications. One installation in the Pittsburgh area is shown in Figure 4. These glass panels are much larger and heavier than the modules (approximately 5 x 7 feet, 1/4 inch thick) and are supported only by the two-component adhesive system. Most of the panels are vertical, but the top course is inclined approximately 15° back from the vertical while the bottom course is inclined the same amount in the opposite sense so that these panels are suspended. This installation was designed to survive an 80 mph wind. This particular installation is four years old and has no indications of damage from wind, winter temperatures as low as -20°F, summer temperatures up to 100°F, and severe rain and snow storms.

### 3. Electrical Design

A second important design innovation is the use of twelve parallel strings of fifteen series connected cells. This is a much higher number of parallel connected strings that is commonly found in photovoltaic modules. This arrangement provides two significant advantages:

- If any single cell becomes a nonconducting cell because of cracking, connection separation, or other open circuit failure, the output of only one series out of twelve is lost. With this arrangement and under the cell failure conditions specified, the module output is reduced only 8.33%. This clearly satisfies the specification of JPL Document 5101-138 which calls for the module output to be reduced no more than 10% under these conditions.

ORIGINAL PAGE  
BLACK AND WHITE PHOTOGRAPH

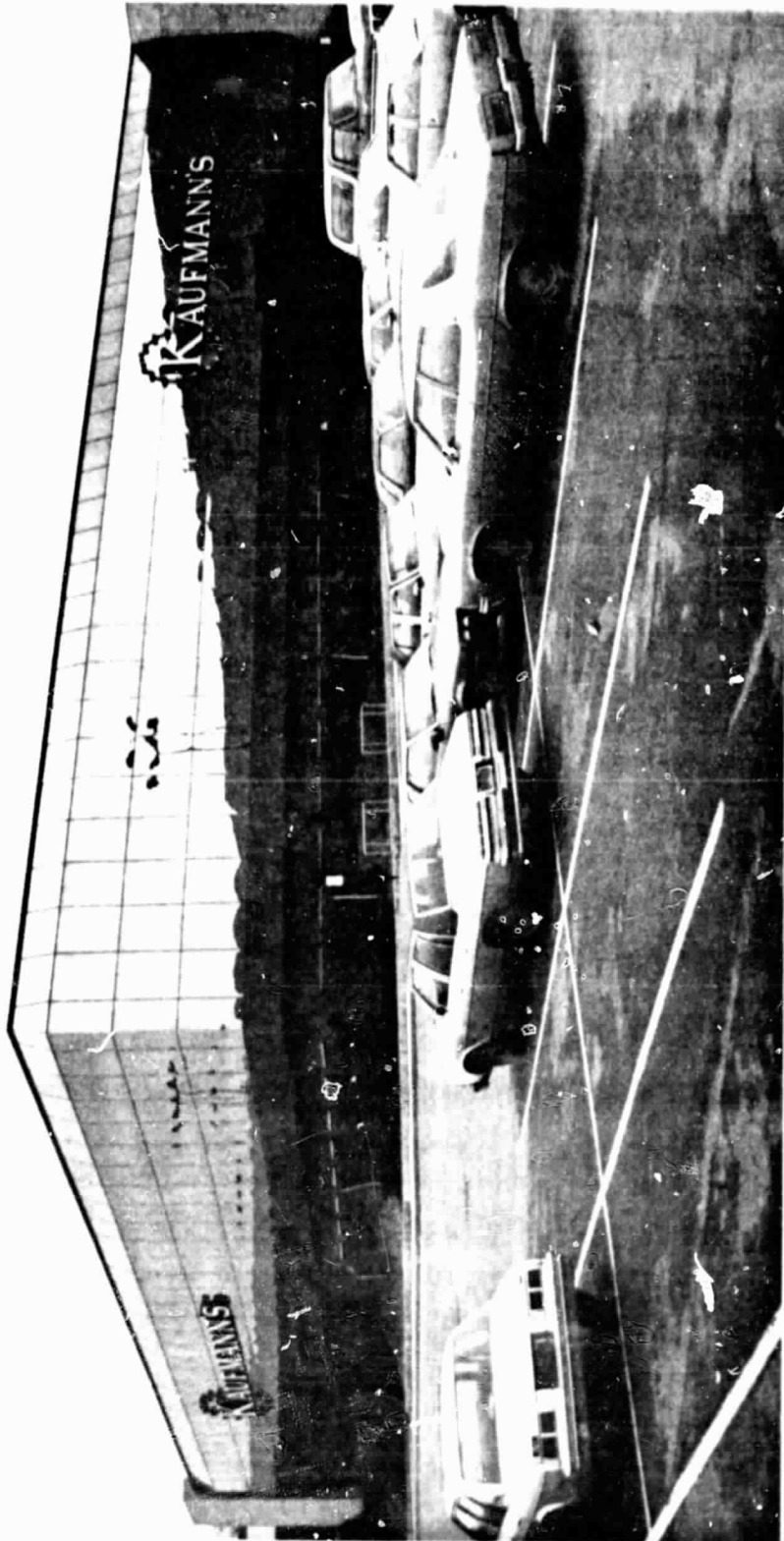


Figure 4. Glass Panelled Wall Utilizing Structural Adhesive Supports

- If any single cell becomes a nonconducting cell because of shading, the potential available to force current through it in its high resistance condition is that produced by only 14 cells. Calculations and tests described below verified that one shaded cell in a series of 15 will survive short circuit operation indefinitely without damage. This design eliminates the need for incorporation of costly blocking diodes to prevent cell damage during short circuit/shaded operation. These diodes have been found to have been the cause of some module field failures.

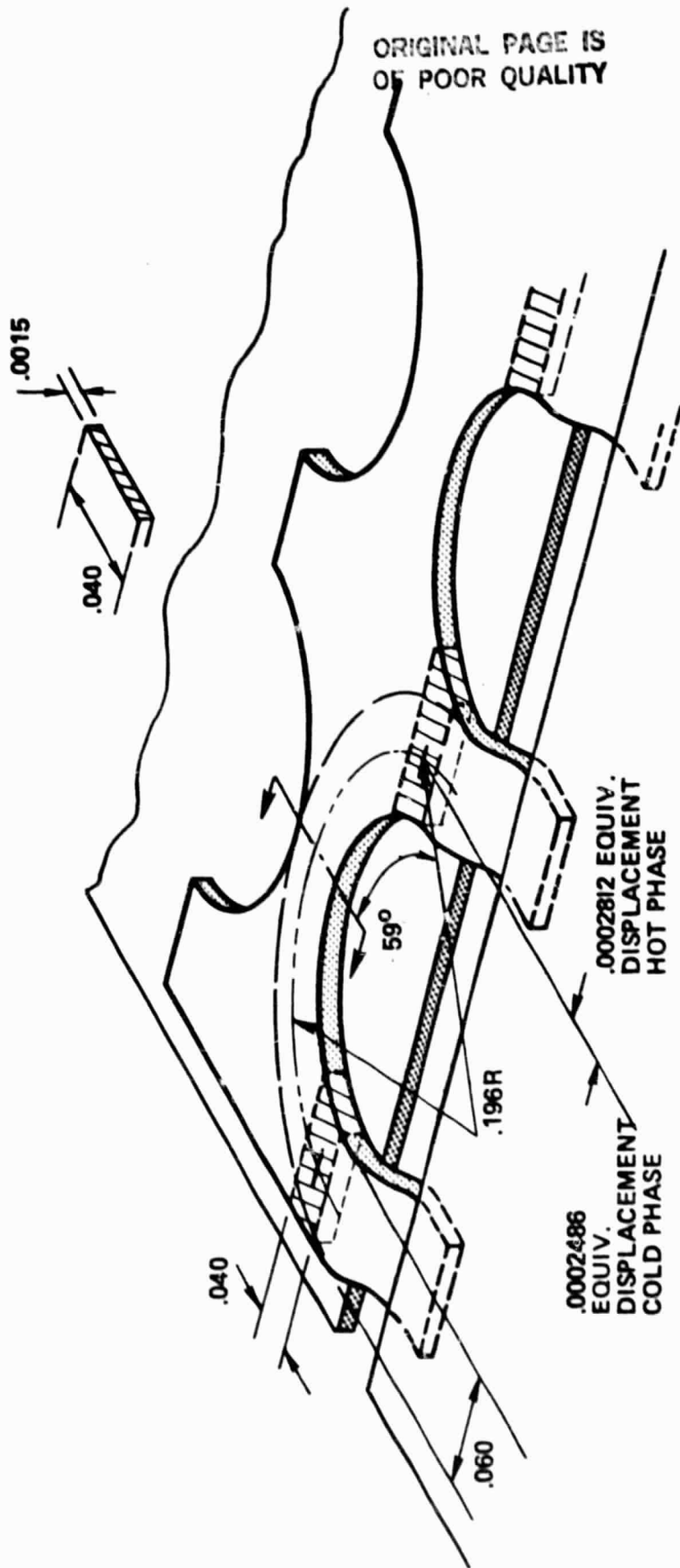
The Westinghouse MEPSDU module is unique in its approach to the electrical interconnection of cells. Each cell has a front surface grid pattern that collects current and directs it to eight .040" x .060" copper interconnect pads evenly spaced near the edge of the long cell dimension. Cell-to-cell interconnection is achieved by bonding .0015 inch thick aluminum foil with circular punched-out holes to the interconnect pads on the front surface of each cell and to the metallized back (dark) side of the adjacent cell. The geometry of the interconnection scheme is shown in Figure 5.

Thus, there are eight individual bonds made to each side of each individual cell providing a higher degree of redundancy than is found in any other photovoltaic module design. Since interconnect failure has been found to be a major cause of module field failures, this redundancy is felt to be highly desirable.

Because of the large number of bonds required in the Westinghouse design, a high speed bonding technique is required. For this reason, an ultrasonic bonding scheme was developed to replace the standard reflow solder joining technique. The ultrasonic bonding technique eliminates cell heating during the bond operation, eliminates flux application and removal requirements and provides substantially improved mechanical and electrical bonds. Automation of the bonding operation is described in a separate section of this report.

The necessity for (or the desirability of) a strain relief, such as an S-bend, in the aluminum electrical interconnections between photovoltaic cells has





705978-1A

Figure 5. Geometry of Ultrasonic Bonds, Dark Side

been a concern often expressed during discussions of the Westinghouse module design. This problem has been examined; and the conclusion of the engineering analysis is that a strain relief is not necessary, and because of the cost of producing it, is not desirable. This conclusion is based upon the following logic:

- The simplified geometry of the interconnection is as shown in Figure 6.
- At some temperature below the lamination temperature of the module (150°C), the ethylene vinyl acetate (EVA) matrix "freezes," i.e., permitting no further relative movement of the unstressed components. This temperature is conservatively assumed to be 90°C, so that stress calculations can be related directly to the thermal cycling of the module between -40 and +90°C. The actual immobilization temperature is probably nearer 64°C, the softening point of EVA, which would reduce the actual thermal strains.
- The coefficients of thermal expansion of the materials involved have the following values:

soda-lime glass	- $8.46 \times 10^{-6}/^{\circ}\text{C}$
aluminum	- $23.6 \times 10^{-6}/^{\circ}\text{C}$
silicon	- $2.9$ to $7.4 \times 10^{-6}/^{\circ}\text{C}$ ; the value $7.4 \times 10^{-6}$ was used in this analysis because it is the less optimistic assumption
- For a cell in a series string with neighbors on both sides, it is assumed that the center of the cell is fixed with respect to the glass superstrate and that differential thermal expansion is permitted by shear deflection of the low-modulus EVA.
- The relative motion of the edges of the ultrasonic welds in the aluminum interconnection during the 130°C temperature excursion from +90°C to -40°C is calculated to be:

ORIGINAL PAGE IS  
OF POOR QUALITY

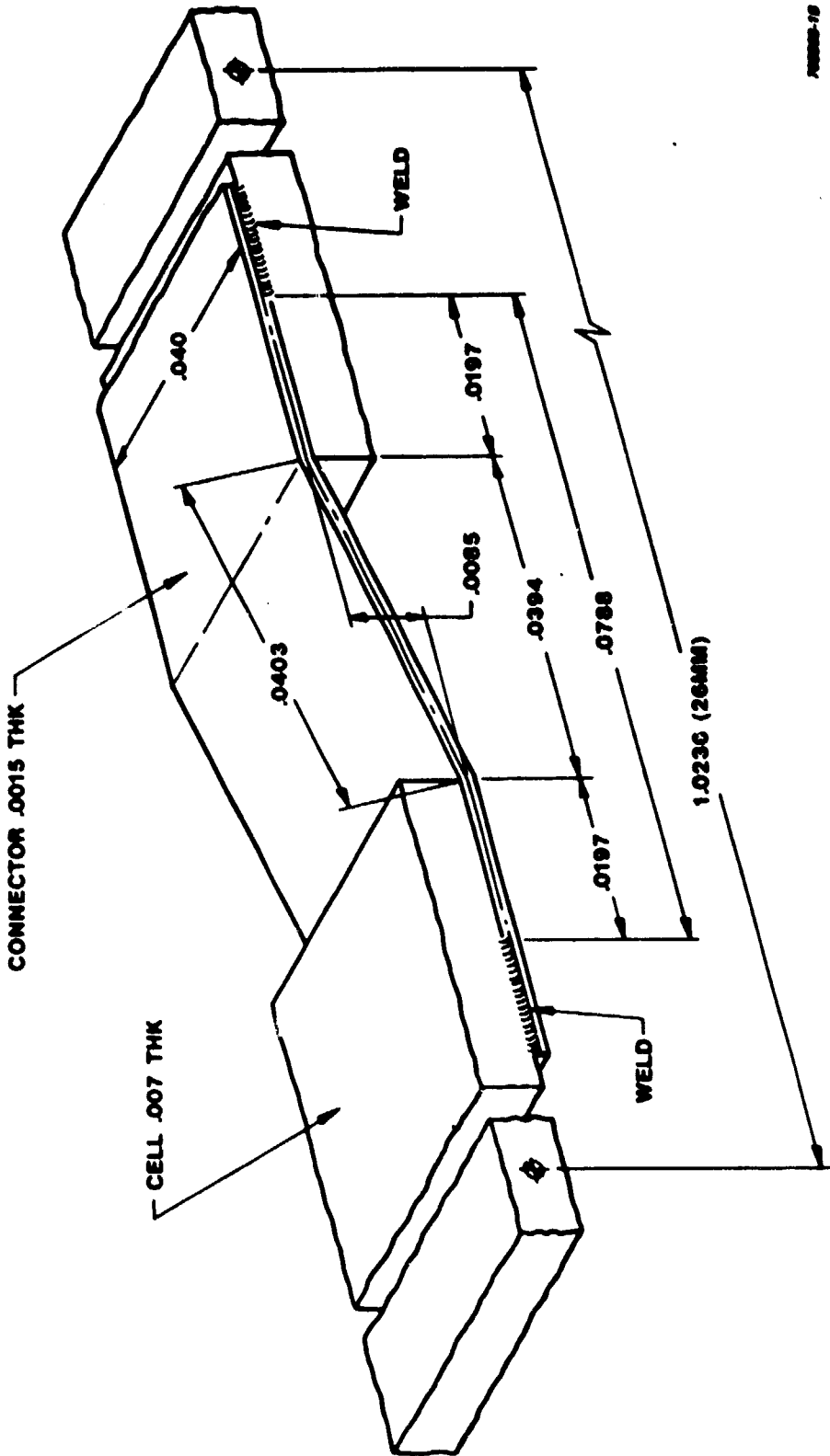


FIGURE 6

Figure 6. Cell Interconnection Geometry

contraction of the glass between centers: 0.00113 inch  
contraction of silicon between centers: 0.000910 inch  
differential motion: .000217 inch

- The calculated contraction of the aluminum between the edges of the welds is 0.000245 inch.
- The extension from its free state of the aluminum between welds is calculated to be 0.0000276 inch. This requires a strain of 0.0346%, which in aluminum results in a tensile stress of 3462 psi. The endurance limit of aluminum alloys 1060-H14 and 1100-0 is  $\pm 5000$  psi.
- The calculated tensile force in the interconnect tab is 0.208 lbs. The shear stress in the ultrasonic weld, if it is a full area weld, is only 129.8 psi, which is negligible. Tear tests of these welds show approximately full coverage welds, whereas calculations show that as little as 10% coverage would be adequate both electrically and mechanically.

A similar type of analysis was performed to study a second interconnect or bond failure mechanism associated with stresses resulting from differential thermal expansion of the cells and interconnects in the parallel direction (ref. Figure 4). The failure mechanism postulated is successive bond failure during the cold phase of the thermal cycles, beginning at the ends of the cell interconnections and proceeding toward the center of the cell as each bond failure causes its inboard neighbor to become the outboard bond, i.e., the bond acted upon by unbalanced forces. This problem has been examined with the conclusion being that this "domino" failure will not occur and the multiple redundant interconnections will survive thermal cycling. This conclusion is based upon the following logic:

- The ultrasonic bonds between the aluminum interconnections and the silicon cells are made with the spans between bonds at room temperature (21°C); thermal cycling between -40°C and +90°C

causes a negative temperature excursion of 61°C and a positive excursion of 69°C.

- The coefficients of thermal expansion of the materials involved have the following values:

aluminum -  $23.6 \times 10^{-6}/^{\circ}\text{C}$

silicon - 2.9 to  $7.4 \times 10^{-6}/^{\circ}\text{C}$ ; the value  $2.9 \times 10^{-6}/^{\circ}\text{C}$  used in this analysis because it is the less optimistic assumption

- During the negative temperature excursion, a thermal strain of  $61 \times (23.6 - 2.9) \times 10^{-6} = 0.001263$  in/in is imposed on the system. It is conservatively assumed that the total strain is imposed on the thin (0.0015") aluminum rather than on the thicker (0.007") and stiffer silicon and that the aluminum provides a direct (straight line) load path between bonds. The calculated equivalent stress for this strain is 16,500 psi tension, greater than the 13,000 psi yield strength reported for aluminum alloy 1060-H14, and much greater than the 5,000 psi reported for 1100-0; the aluminum would therefore yield. During the positive temperature excursion, the aluminum, because of its higher coefficient of thermal expansion, would expand more rapidly than the underlying silicon, so that the tensile load would drop to zero. Compressive loading of the aluminum foil will be very slight because the low elastic modulus of the ethylene vinyl acetate clamping the aluminum to the silicon will permit rippling of the aluminum; but upon recooling, the aluminum will again be stressed to its yield strength. An in-line load path in the aluminum between ultrasonic bond pads must therefore be avoided.
- The actual geometry of the aluminum interconnection and the silicon cell is shown in Figure 5.

- Differential strain of the aluminum and silicon can be accommodated by flexure of the aluminum "arch" at its minimum section height. Flexure would occur during both the positive and negative temperature excursions. The greater differential strain occurs during the 69°C positive excursion and is 0.00143 in/in. If each half-arch is considered to be a fixed end beam with a tip load sufficient to produce a deflection equivalent to the restraint, the equivalent deflection is .00714 mm or 0.00028 inches. The stress produced by this deflection of the tip of an equivalent cantilever beam at its point of zero deflection (the peak of the arch) is 4106 psi. The corresponding stress during the negative temperature excursion is 3630 psi. Both of these values are less than 5000 psi, the endurance limit (the stress at which an unlimited number of stress reversals can be survived) of aluminum alloys 1060-H14 and 1100-0. Either of these alloys is satisfactory - the selection to be based on mechanical handling of the interconnections during processing. To produce this stress in the interconnections, the shear stress in the end bonds, if these are 0.040" x 0.040", is only 5.06 psi.

#### B. Module Performance Evaluation

Performance evaluation of the prototype MEPSDU module was completed prior to fabrication and testing of a prototype module. Calculations were based on a cell of the dimensions specified in the module drawing package (2.5 cm x 9.83 cm x 0.015 cm) and having the following performance characteristics at AM1, 100 mW/cm<sup>2</sup> and 25°C:

Short circuit current density = 0.031 A/cm<sup>2</sup>

Open circuit voltage = 0.580 V

Fill Factor = 78 percent

Efficiency = 14.0 percent

Dendritic web cells which have been manufactured on the Westinghouse Pre-Pilot Facility using the MEPSDU process sequence have routinely displayed these performance characteristics.

Encapsulation thicknesses and materials in the Westinghouse prototype MEPSDU module are as shown in Figure 7. The calculations were performed using a cell-to-still-air thermal impedance of  $300^{\circ}\text{Ccm}^2/\text{W}$ . This thermal impedance was determined experimentally using a small (5" by 8") encapsulated "minimodule" having the MEPSDU module layout configuration. An optical transmission factor of .96 (taken from "Sunadex" glass literature) and an electrical mismatch factor of .98 were assumed for the calculations. A packing factor of .92 was used in the calculations as determined from cell and module dimensions contained in the module drawing package.

Figures 8 and 9 present four significant calculated module parameters: open circuit voltage ( $V_{oc}$ ), short circuit current ( $I_{sc}$ ), efficiency, and power output, all plotted as functions of ambient air temperature for operation at AM1,  $100 \text{ mW/cm}^2$ . Note that the open circuit voltage and short circuit currents of the MEPSDU module have nearly the same absolute value (approximately 8.5 volts and 8.5 amps). This is a result of the specific series/parallel circuit configuration chosen for the module.

Table 5 summarizes the calculated performance parameters for the Westinghouse MEPSDU module at both standard operating conditions ( $80 \text{ mW/cm}^2$  insolation and  $20^{\circ}\text{C}$  ambient temperature) and at standard test conditions ( $25^{\circ}\text{C}$  cell operating temperature and  $100 \text{ mW/cm}^2$  insolation level). The latter case defines operating conditions under which the 1986 LSA cost objectives have been defined. The calculated efficiency level of 12.3% exceeds the 12.0% level assumed in the economic analysis presented in a later section of this report.

Figure 10 presents an actual I-V test curve for a recent prototype MEPSDU module fabricated on the Westinghouse Pre-Pilot Facility using cells produced by the baseline MEPSDU process sequence. This module, Model #AESD-1, S/N-18, differs from the prototype MEPSDU module in that the cells used in the module were 2.0 cm x 9.8 cm as opposed to the MEPSDU design of 2.5 cm x 9.83 cm. As a result, the S/N-18 module has 12 parallel strings of cell, each string containing 18 rather than 15 cells. The overall module area of the S/N-18 module is  $4560 \text{ cm}^2$  rather than  $4760 \text{ cm}^2$ . This change modifies the I-V characteristic

ORIGINAL PAGE IS  
OF POOR QUALITY

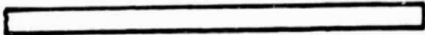






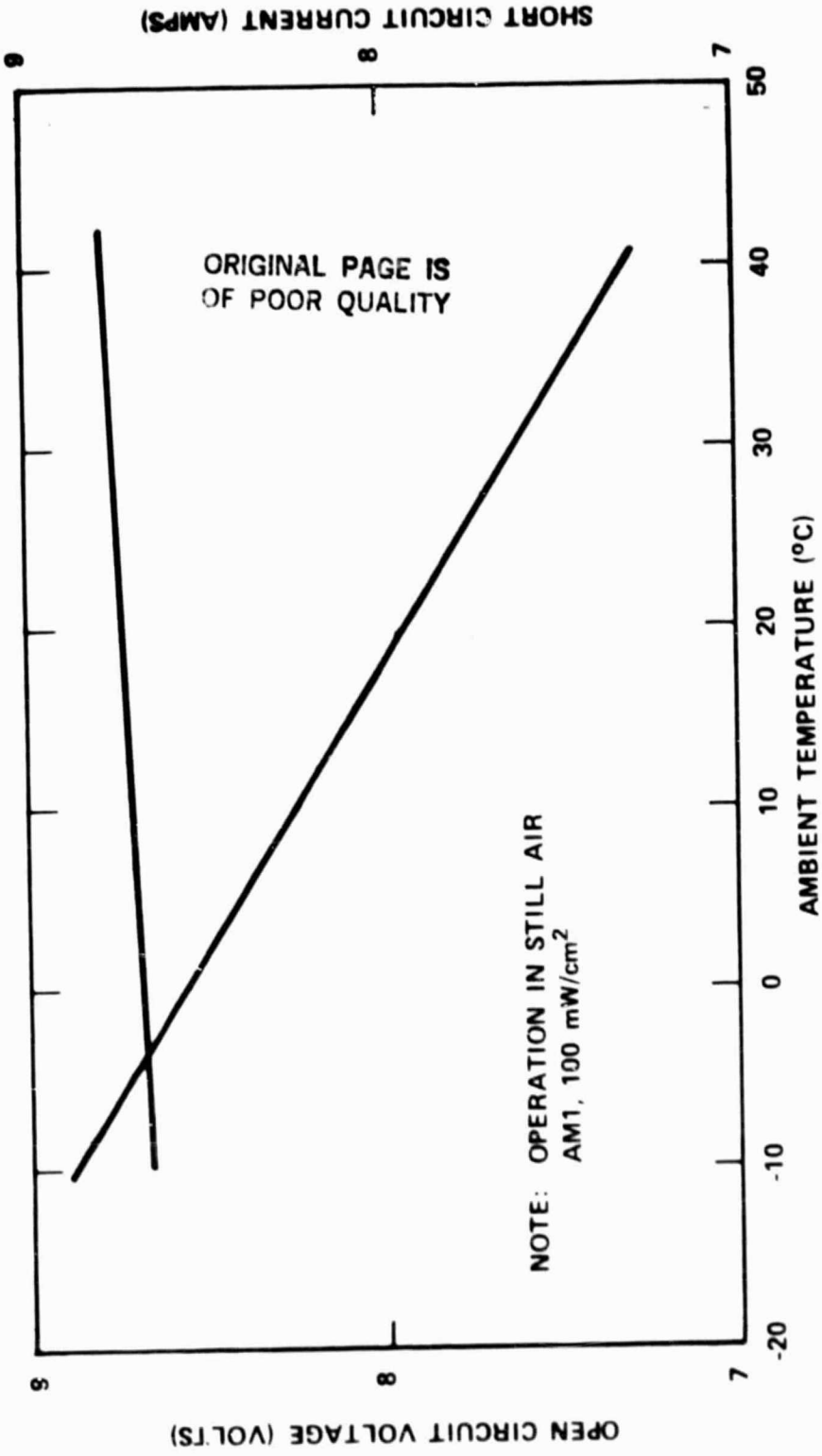
		<u>Thickness</u>	
		<u>cm.</u>	<u>in.</u>
	Tempered Glass	.318	.125
	Craneglas	.013	.005
	EVA	.050	.020
	Solar Cells	.015	.006
	EVA	.050	.020
	Craneglas	.013	.005
	Mylar (Korad)	.007	.003

Figure 7. Layup Materials and Dimensions of the Westinghouse MEPSDU Module

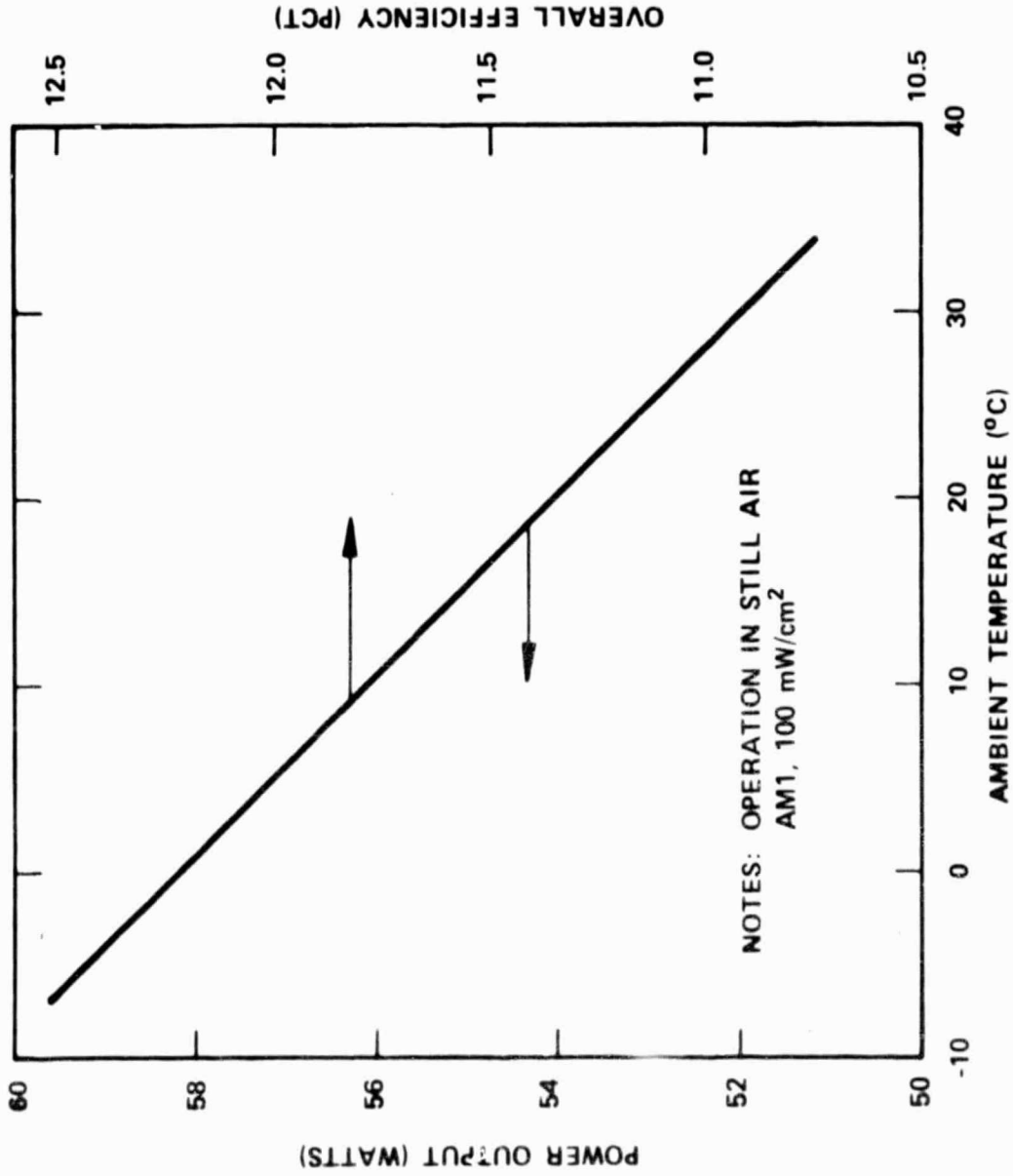




706511-3A

Figure 8. Calculated MEPSDU Module  $V_{oc}$  and  $I_{sc}$  as Functions of Ambient Temperature

ORIGINAL PAGE IS  
OF POOR QUALITY



706511-2A

Figure 9. Calculated MEPSDU Module Power and Efficiency as Functions of Ambient Temperature

ORIGINAL PAGE IS  
OF POOR QUALITY

TABLE 5

CALCULATED MEPSDU MODULE PERFORMANCE PARAMETERS

<u>Parameter</u>	<u>Standard Operating Condition (1)</u>	<u>Standard Test Condition (2)</u>
Open Circuit Voltage	8.08 volts	8.61 volts
Nominal Operating Voltage	6.57 volts	7.00 volts
Short Circuit Current	6.98 amps	8.69 amps
Nominal Operating Current	6.70 amps	8.35 amps
Peak Power	44.0 watts	58.4 watts
Efficiency at Peak Power	11.6 pct	12.3 pct

(1) Standard Operating Conditions: 20°C ambient air temp, insolation =  
80 mW/cm<sup>2</sup>

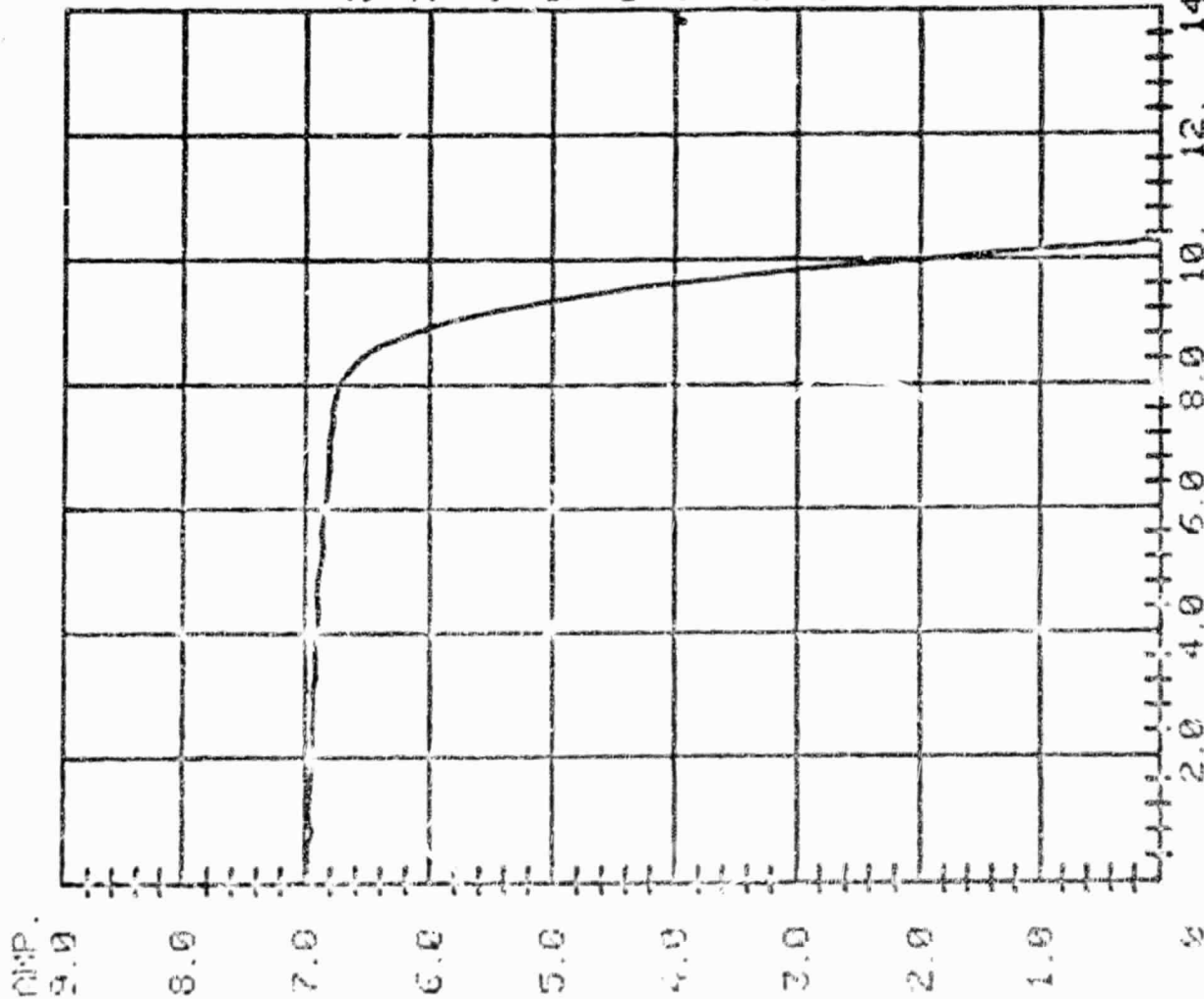
(2) Standard Test Conditions: 25°C cell temperature, insolation =  
100 mW/cm<sup>2</sup>

ORIGINAL PAGE IS  
OF POOR QUALITY

S P E C T R O L A B

MODEL # AESD-1  
SERIAL # 0018  
DATE 5/4/82

- 1 CELL AREA (SQ MM) 1960
  - 2 # OF CELLS IN PARALLEL 12
  - 3 # OF CELLS IN SERIES 18
  - 4 AMBIENT TEMP (DEG C) 21
  - 5 STANDARD TEMP (DEG C) 25
  - 6 I TEMP COR(UA/SQ CM/DEG C) 25
  - 7 V TEMP COR(UV/DEG C/CELL) -2200
  - 8 AM1 CAL CURRENT (0.1'S MA) 1093
  - 9 TEST VOLTAGE (0.01'S V) 45
  - 10 MIN I(TEST) (0.01'S A) 5
- I(TEST) = 7009000 UA  
ISC = 6972000 UA  
VOC = 10258000 UV  
MAX POWER 55336327 UN  
@ 8628000 UN /A



$$\eta = \frac{55}{456} = 12.14\%$$

Figure 10. I-V Test Curve of Prototype MEPSDU module

of the module and reduces the expected output power by 4.2 percent - the ratio of the module areas; but the efficiency and temperature characteristics are essentially identical to those of the MEPSDU module. Note that efficiency of the S/N-18 test module, 12.1 percent, also exceeds the 12 percent level assumed in the economic analysis presented in a later section of this report.

### C. Environmental Testing

#### 1. Hailstone Impact Tests

Two full-size simulated modules, laminated and bonded to test frames\* using the adhesive configuration specified by the Westinghouse MEPSDU module interface drawing, were delivered to JPL in November 1981 for high velocity iceball impact tests as specified by JPL Document 5101-138. Preliminary testing conducted at Westinghouse indicated that the 1/8" thick tempered glass module superstrate can survive the hailstone impact tests.

Testing was completed by JPL personnel in December 1981, and both modules passed all phases of the test. It should be noted that, in addition to the 1" diameter hailstones specified by 5101-138, both modules also passed the 1 1/4" and 1 1/2" diameter hailstone tests. All of the tests were conducted using terminal velocities associated with each size hailstone. Thus the 1 1/2" diameter hailstone impacted the glass superstrate with an energy content five times that of the JPL 5101-138 requirement.

#### 2. Wind Load Testing

Tests were conducted by Westinghouse to demonstrate that the 1/8 inch tempered glass superstrate and encapsulated cells of the prototype MEPSDU module can survive both positive and negative wind loading conditions specified by JPL Document 5101-138.

---

\*This test frame supports the module and takes the place of the support structure in the deployed array. The frame does not protect the edges of the module.

For the positive wind loading test, the module edge support load equivalent to 125% of the design wind load was transmitted through elastomeric material overlapping the ends of the cells varying amounts, up to 3/8 inch. No damage to the superstrate or any of the cells was observed.

The simulated negative wind loading test, designed to simulate wind loads which would tend to lift the module off its edge support (thus placing the structural adhesive attachment in tension), was also successfully performed. The test was conducted on a frameless minimodule that was attached to a support by the double-faced polyurethane tape and silicone structural adhesive with which the modules will be mounted in test and service installations. The back face of the minimodule was loaded by a uniformly distributed layer of fine tungsten powder (enclosed in a thin plastic bag and restrained laterally by vertical plastic dams). The depth of the tungsten powder, 9 inches, was sufficient to develop a restraining tensile force of 25 lbs per linear foot of the module edge, applied to the module through the structural adhesive bond to the back face of the module encapsulation. This tensile force is the same as a  $50 \text{ lb/ft}^2$  wind load will develop on a full-size module. The load was sustained for fifteen minutes, rather than for one minute as the specified gust loading, with no indications of tearing, separation, or creep in the support attachment.

### 3. Thermal and Humidity Cyclic Tests

Twelve small modules were assembled for environmental testing. These modules were made to evaluate several different layups, substitutes for Korad-KLEAR as the back surface weather seal, and Tedlar tape as an edge seal. Cells with efficiency levels unacceptably low for incorporation into modules were selected for use in these tests. Cut window glass was used on all the test modules rather than tempered float glass which will be used on the MEPSDU modules. The layup of each of these modules is shown in Table 6.

The following comments are made in regard to the appearance of the as-laminated modules. The sun side of module G-2 was clearer than the modules that had a layer of Craneglas between EVA and the window glass. The back surfaces of modules with Korad back covers (G-1, G-2, G-3, G-10, G-11, and G-12) were

TABLE 6

LAYUP OF SMALL MODULES USED FOR ENVIRONMENTAL TESTING

G-1	G-2	G-3	G-4	G-5	G-6
(1.6 x 9.4 cm cells) Window Glass Craneglas EVA 5 Cell String Craneglas EVA Craneglas Korad-KLEAR	(1.6 x 9.4 cm cells) Window Glass EVA 5 Cell String Craneglas EVA Craneglas Korad-KLEAR Tedlar Edge Tape	(1.6 x 9.4 cm cells) Window Glass Craneglas EVA 5 Cell String Craneglas EVA Craneglas White Korad	(1.6 x 9.4 cm cells) Window Glass Craneglas EVA 5 Cell String Craneglas EVA Craneglas Clear Tedlar (2 mil) Tedlar Edge Tape	(1.6 x 9.4 cm cells) Window Glass Craneglas EVA 5 Cell String Craneglas EVA Craneglas Clear Tedlar (4 mil)	(1.6 x 9.4 cm cells) Window Glass Craneglas EVA 5 Cell String Craneglas EVA Craneglas White Tedlar (2 mil)
G-7	G-8	G-9	G-10	G-11	G-12
(1.6 x 9.4 cm cells) Window Glass Craneglas EVA 5 Cell String Craneglas {EVA Primed Clear Tedlar (2 mil)}	(1.6 x 9.4 cm cells) Window Glass Craneglas EVA 5 Cell String Craneglas {EVA Primed White Tedlar (2 mil)}	(1.6 x 9.4 cm cells) Window Glass Craneglas EVA 5 Cell String Craneglas EVA Craneglas Acrylar X-22417 Tedlar Edge Tape	(1.2 x 10 cm cells) Window Glass Craneglas EVA 5 Cell String EVA Craneglas White Korad	(1.2 x 10 cm cells) Window Glass Craneglas Elvax 5 Cell String Elvax Craneglas White Korad	(1.2 x 10 cm cells) Window Glass Craneglas EVA 7 Cell String* EVA Craneglas Korad-KLEAR

\*K&S bonded

wrinkled transverse to the long direction of the cells. The back surfaces of modules made with .002 inch thick Tedlar back covers (G-4, G-6, G-7, and G-8) were fairly smooth. The .004 inch thick Tedlar back cover of module G-5 was extremely smooth. The use of EVA primed Tedlar (G-7 and G-8) simplified the layup. The Acrylar back cover of module G-9 was extremely wrinkled with a random orientation. The use of Elvax\* (non-blocking EVA) in module G-11 produced no noticeable difference in lamination or module performance. Because it is non-blocking, it is much easier to handle. The elimination of Craneglas behind the cell string in modules G-10, G-11, and G-12 also had no adverse effect on either appearance or performance. The white back covers made it possible to observe shrinkage/wrinkling effects that suggest that all back cover materials should be cut slightly oversize prior to lamination. The shrinkage/wrinkling effects were not easily detected with clear back covers because of the transparency of all of the films used in the layups. The cut window glass did not have an edge of the quality of manufactured tempered float glass; therefore, the Tedlar tape edge seal did not "corner" well on all sides of modules G-2, G-4, and G-9.

A typical test module is shown in Figure 11, and the twelve test modules are shown loaded in a test fixture in Figure 12.

Because of a malfunction of the test equipment, pre-lamination measurements made on cell strings for modules G-1 through G-9 were not valid. However, pre- and post-lamination measurements were obtained on the cell strings in modules G-10, G-11, and G-12; and these data are shown in Table 7. The differences seen in the data are within the measurement error of our equipment; and the effect, if any, of the laminating materials or process upon cell or module characteristics is minimal.

All twelve modules were placed in an environmental test chamber and subjected to the thermal cycles specified in JPL 5101-138, Figure 5.1. (Due to equipment

---

\*DuPont Trade Name



ORIGINAL PAGE IS  
OF POOR QUALITY

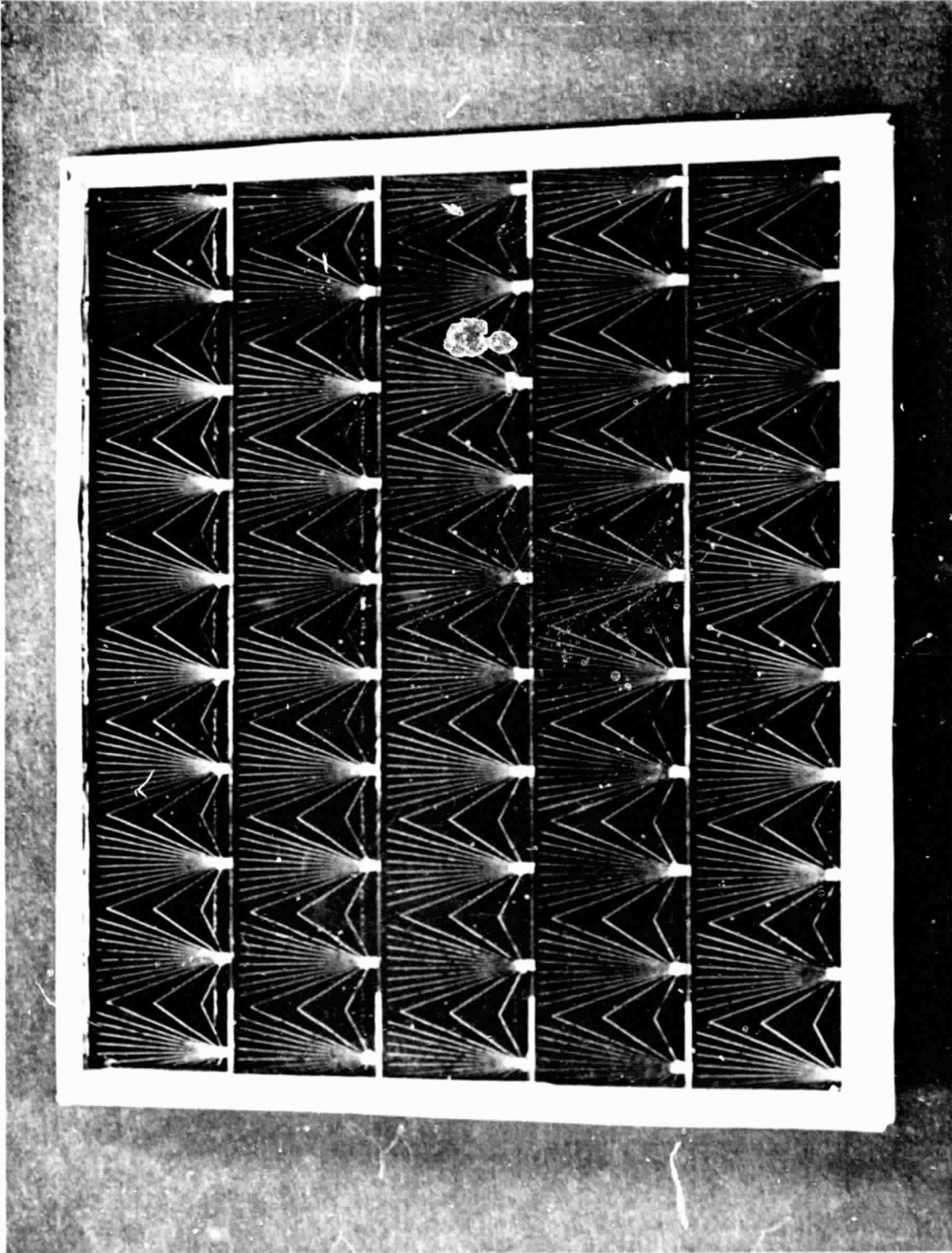


Figure 11. Environmental Test Module G-2 (10 cm x 9 cm)

ORIGINAL PAGE IS  
OF POOR QUALITY

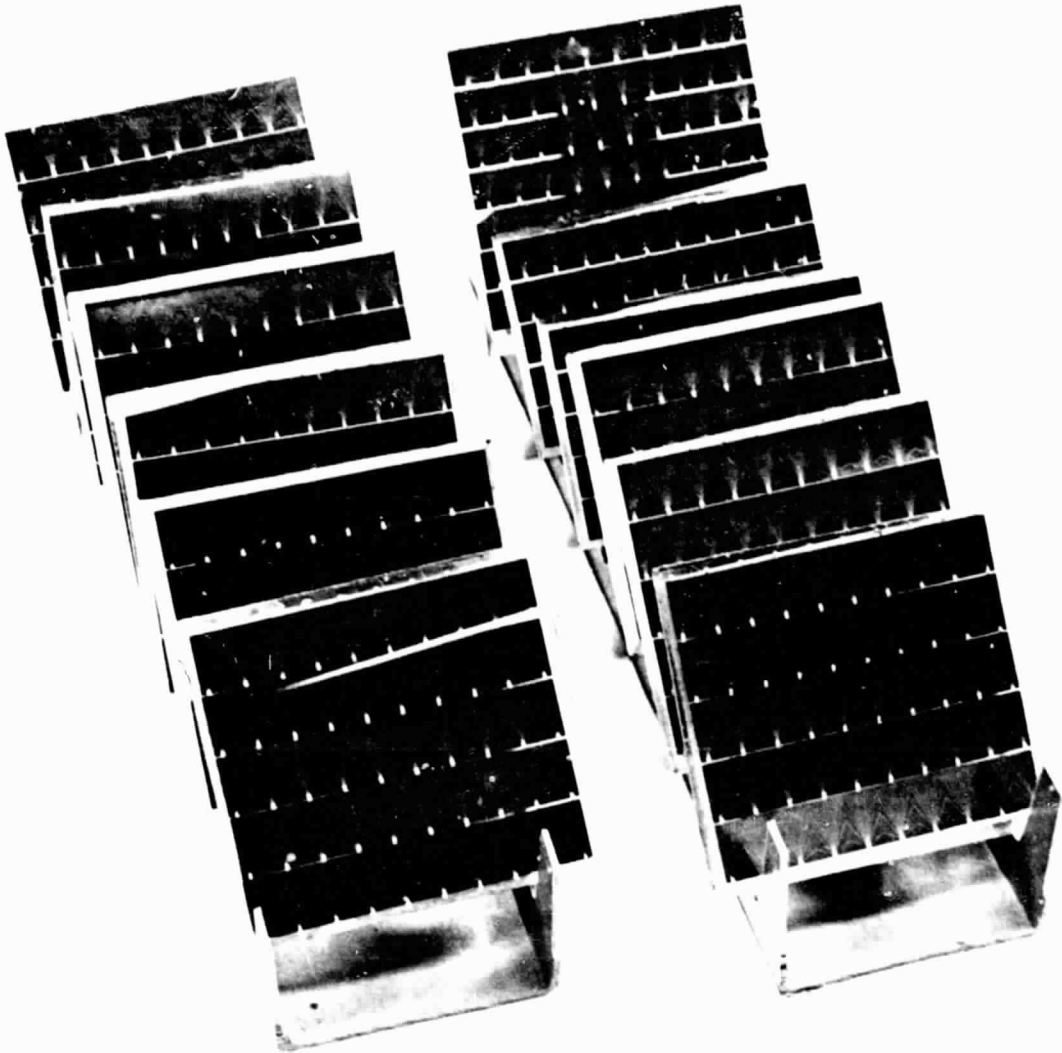


Figure 12. Environmental Test Modules in Humidity Test Fixture

TABLE 7

PRE- AND POST-LAMINATION MEASUREMENTS OF CELL STRING CHARACTERISTICS

Module No.	Pre-Lamination Cell String Characteristics			Laminated Module Characteristics		
	Voc (V)	Isc (A)	FF (%)	Voc (V)	Isc (A)	FF (%)
G-10	2.60	.298	.77	2.66	.283	.77
G-11	2.52	.309	.74	2.69	.295	.75
G-12	3.58	.297	.73	3.75	.273	.75

NOTE: All cells used in the assembly of these test articles were produced during early checkout operations on the Westinghouse pre-pilot facility. These efficiency levels are not representative of the pilot line or the MEPSDU process sequence.

ORIGINAL PAGE IS  
OF POOR QUALITY

limitations, the minimum temperature achievable in these tests is  $-35^{\circ}\text{C}$  as opposed to the specified level of  $-40^{\circ}\text{C}$ ). Open circuit voltage and short circuit current measurements were made on each of the modules after lamination, after completion of 25 cycles, and again after completion of 50 cycles. These data are given in Table 8. As before, the differences seen in the data are within the measurement error of the equipment. The effect, if any, of the thermal cycling test upon cell or module characteristics is not measurable.

Each of the modules was examined after the thermal cycling test. There was some separation of the lamination from the glass on modules G-1, G-3, and G-5 and some debonding of the edge tape from the glass on module G-2. These were random effects and could not be correlated to materials or processes. They were noted, however, because it was felt that the separation may permit ingress of moisture by a route other than permeation through the lamination films during subsequent humidity tests.

All twelve small modules were then placed in an environmental test chamber and subjected to the humidity test conditions defined by JPL 5101-138, Figure 5.2. The modules were inclined at  $45^{\circ}$  during the test. The modules and the holding fixture were shown previously in Figure 12.

Open circuit voltage and short circuit current measurements were made on each of the modules within one-half hour after the completion of the humidity test. These data are compared to data obtained as-laminated and after 50 thermal cycles in Table 9. Differences seen in the data are within the measurement error of the equipment. The differences, if any, on the performance characteristics of the small modules subjected to the environmental tests specified in JPL 5101-138 are not measurably significant.

A re-examination of each of the modules after the humidity test indicated that, except for a slight darkening of the external copper leads, there was no noticeable change in the appearance of the modules as a result of the humidity test.

TABLE 8

## MEASUREMENTS MADE ON THERMALLY CYCLED TEST MODULES

Module No.	Open Circuit Voltage			Short Circuit Current		
	As Laminated	After 25 Cycles	After 50 Cycles	As Laminated	After 25 Cycles	After 50 Cycles
G-1	2.58	2.61	2.52	.318	.340	.337
G-2	2.58	2.62	2.60	.278	.295	.285
G-3	2.57	2.63	2.61	.326	.351	.345
G-4	2.46	2.61	2.60	.330	.339	.330
G-5	2.48	2.53	2.52	.246	.266	.256
G-6	2.52	2.58	2.57	.262	.281	.272
G-7	2.51	2.55	2.57	.265	.280	.271
G-8	2.54	2.59	2.60	.267	.288	.283
G-9	2.58	2.63	2.64	.330	.346	.335
G-10	2.66	2.68	2.69	.283	.303	.294
G-11	2.69	2.71	2.71	.295	.309	.299
G-12	3.75	3.77	3.75	.273	.283	.272

ORIGINAL PARTS  
OF POOR QUALITY

ORIGINAL PAGE IS  
OF POOR QUALITY

TABLE 9  
MEASUREMENTS MADE ON ENVIRONMENTAL TEST MODULES

Module No.	Open Circuit Voltage			Short Circuit Current		
	As Laminated	After 50 Thermal Cycles	After Humidity Test	As Laminated	After 50 Thermal Cycles	After Humidity Test
G-1	2.58	2.52	2.56	.318	.337	.338
G-2	2.58	2.60	2.60	.278	.285	.301
G-3	2.57	2.61	2.62	.326	.345	.338
G-4	2.46	2.60	2.60	.330	.330	.335
G-5	2.48	2.52	2.53	.246	.256	.258
G-6	2.52	2.57	2.58	.262	.272	.277
G-7	2.51	2.57	2.56	.265	.271	.272
G-8	2.54	2.60	2.60	.267	.283	.277
G-9	2.58	2.64	2.64	.330	.335	.333
G-10	2.66	2.69	2.70	.283	.294	.292
G-11	2.69	2.71	2.72	.295	.299	.294
G-12	3.75	3.75	3.80	.273	.272	.272

After completion of the humidity tests, the thermal cycle tests were repeated in three sets of 50 cycles, with data being recorded after completion of each set.

Figure 13 shows the measurement of the performance characteristics before and after the series of events occurring from lamination through the completion of 200 thermal cycles for minimodule G-2. This module, with the exception of an added layer of Craneglas over the cells that was found to be unnecessary, is representative of the MEPSDU module layup. The data shown in Figure 13 is typical of the data obtained on the other minimodules in that the modules have exhibited no performance or visual sensitivity to sustained environmental testing.

#### 4. Loss of Cell Contact Pad Electrical Connection

Front surface (sun side) current collection from cells incorporated in the Westinghouse MEPSDU module design is achieved with a series of very fine (1 mil wide) straight conductors emanating from contact pads along one edge of each cell. Cell-to-cell electrical interconnection is achieved by bonding aluminum conductors to each of the contact pads. The fine lines are parallel connected on the surface of the cell so that if the electrical connection to a pad fails, the photocurrent can be collected by neighboring pads albeit with a somewhat higher resistance. This redundancy of contacts leads to a high tolerance for interconnect failure.

To quantify the effect of interconnect failure, several tests were made where the change in the cell output power was determined as a function of the number of pads contacted. At the time these tests were conducted, each cell contained ten interconnect pads located near the long edge of one side of the front surface of the cell.

To carry out the test, cell parameters were first measured with all 10 interconnect pads contacted. The test was then repeated 7 times with the number of pads contacted being reduced by 1 in each test. Table 10 shows the cell design and the results of this experiment. The first three columns of Table 10 show which pads were contacted during each test: the last column shows the output power of the cell at the test conditions.

ORIGINAL PAGE IS  
OF POOR QUALITY

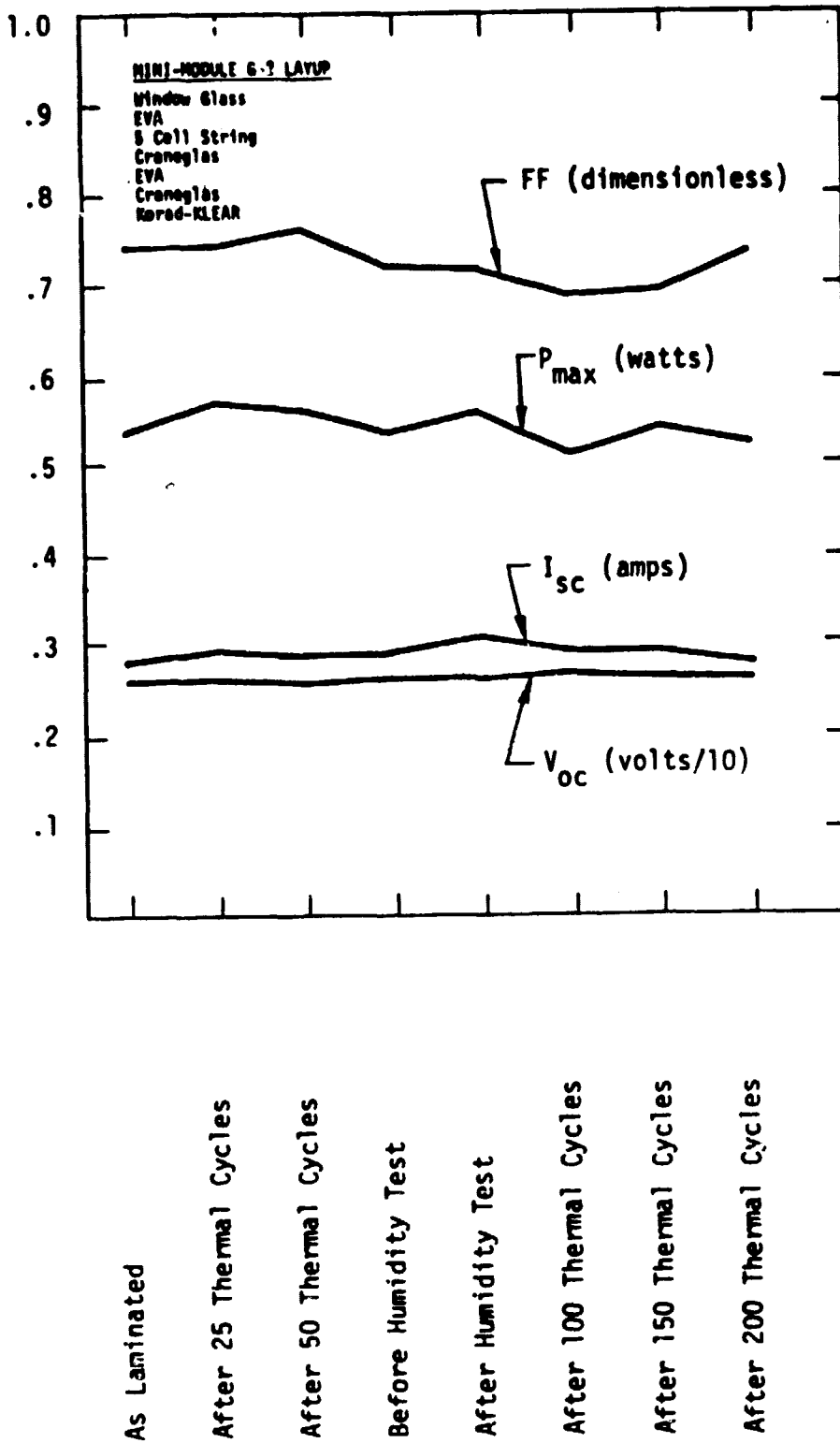


Figure 13. Environmental Test Data from Minimodule G-2



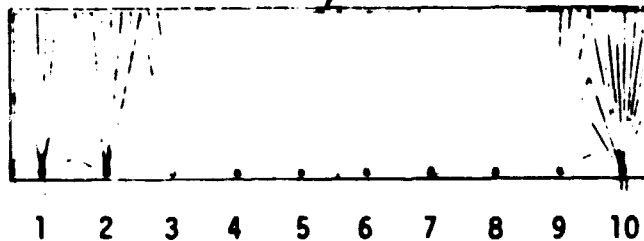
ORIGINAL PAGE IS  
OF POOR QUALITY

TABLE 10

OUTPUT POWER FROM SOLAR CELL AS FUNCTION  
OF INTERCONNECT PADS CONTACTED

<u>Test #</u>	<u>No. of Pads Contacted</u>	<u>Pad No. Contacted*</u>	<u>Cell Power - Out (watts)</u>
1	10	1,2,3,4,5,6,7,8,9,10	0.162
2	9	1,2,3,4,5,6,7,8,9	0.158
3	8	2,3,4,5,6,7,8,9	0.152
4	7	2,3,4,5,6,7,9	0.152
5	6	2,4,5,6,7,9	0.146
6	5	2,4,5,7,9	0.145
7	4	4,5,7,9	0.117
8	3	4,5,7	0.087

\*Pad No. Definition



The power decreased by only 3% when nine pads were contacted and by 7% with only seven pads contacted. With only three pads connected, the power decreased by less than 50%. The major causes of the power loss were the decrease in the fill factor and short circuit current due to the added series resistance of the cell. The thin grid lines in this experiment were conducting the photocurrent over several centimeters, thereby increasing the resistance.

The results given would change if different sequences of pad numbers were contacted. For example, the power output when pads 4, 5, and 6 were contacted would be greater than if pads 1, 2, and 3 were contacted.

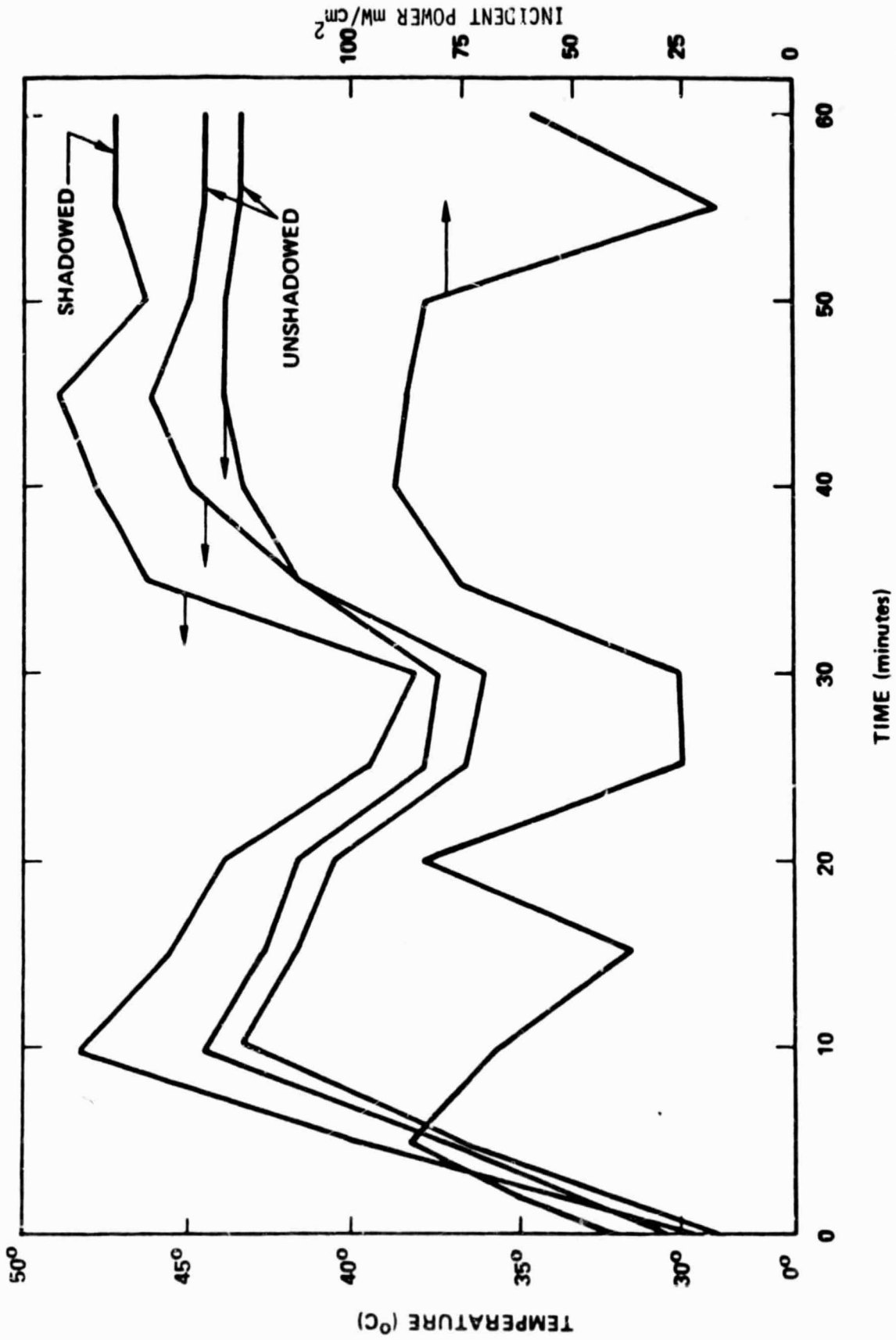
These data, however, do show that several interconnection contacts can be lost in a cell without significantly decreasing the power; and thus the cell design does show a high tolerance for interconnect failure. The results of these tests indicated that the ten pad configuration contained an over-redundancy, and the cell number of interconnect pads on each cell was reduced from ten to eight. This reduction reduces the time required to complete the interconnect bonding operation.

#### 5. Cell Shading Tests

The ability of the prototype MEPSDU solar cell string to survive the short circuit/shaded cell tests specified in JPL Document 5101-138 was questioned by JPL personnel at the Module Design Review. Subsequently, cell shading tests were performed using the 5 cell modules (1.6 cm cells) that were prepared for environmental testing. Three of these modules were connected in series to simulate the 15 cell string of the MEPSDU module. Each cell was then shaded, one at a time, with the modules operating in normal sunlight conditions. Figure 14 shows the test system used for the shading tests. Figure 15 shows the change in temperature (measured on the back cover behind each of the cells) with time and incident power for a test in which the center cell of each 5 cell module of the 15 series connected cells was monitored. Both the shadowed and unshadowed cells responded to changes in incident power, and progressive overheating of the shadowed cell did not occur. In fact, in some tests the shadowed cell ran slightly cooler for corresponding insolation values than it did in the unshaded condition.



Figure 14. Test System Used for Cell Shading Tests



705023-7A

Figure 15. Shadowed Cell Heating Effects under Module Short Circuit Conditions

Further tests were then performed using a continuous 15 cell string of 2.5 cm cells in a layup precisely duplicating the electrical circuit of the MEPSDU module. In these tests, cells were fully shaded and also partially shaded. The results were essentially identical, i.e., no measurable increase in temperature was observed in any shaded condition.

These data reinforce the conclusions that were presented at the Module Design Review: destructive overheating of a shaded cell during short circuit operation of a module is not a problem with the Westinghouse MEPSDU module circuit configuration containing 12 strings of 15 series connected cells. Hence, no internal blocking diodes are required in this module.

## V. PROCESS SEQUENCE DESIGN

### A. Baseline Process Sequence

A baseline process sequence for the fabrication of dendritic web silicon into solar cells and modules was specified during the program. Most of the process steps are based on well-known industrial semiconductor practice that have, in some cases, been modified to take advantage of the unique properties of dendritic web silicon, such as thinness, smooth surfaces, long lengths, etc. These features permit economical fabrication of solar modules.

The cost factors associated with each step of the Westinghouse baseline process sequence have been determined in an economic analysis which is discussed in detail in a later section of this report. Using SAMICS methodology, it has been determined that the specified process sequence can meet the DOE/JPL overall cost objectives of producing photovoltaic modules for 70¢/peak watt in 1986 (1980\$) using large scale manufacturing techniques.

The overall Westinghouse Baseline Process Sequence is outlined in Figure 16. Whereas this figure shows each of the basic operations required to transform dendritic web sheet material into photovoltaic modules ready for shipment, subdividing the process sequence into a series of unit operations is necessary to analyze the process as required to perform economic analyses.

The Westinghouse Baseline Process Sequence flow chart, depicting unit operations, is shown in Figure 17. The sequence is as follows:

1. Pre-Diffusion Cleaning - This consists of a hydrofluoric acid dip, rinse, dry sequence followed by a  $CF_4/O_2$  plasma etch.
2. Front and Back Surface Junction Formation and Oxide Etch - The back surface junction is formed first by applying an  $SiO_2$  layer to the sun side of cleaned web, removing splatter traces of  $SiO_2$  from the back surface with a hydrofluoric acid dip/rinse/dry sequence, diffusing boron into the clean silicon surface, and then removing the boron glass in a hydrofluoric acid dip/rinse/dry sequence. This process is

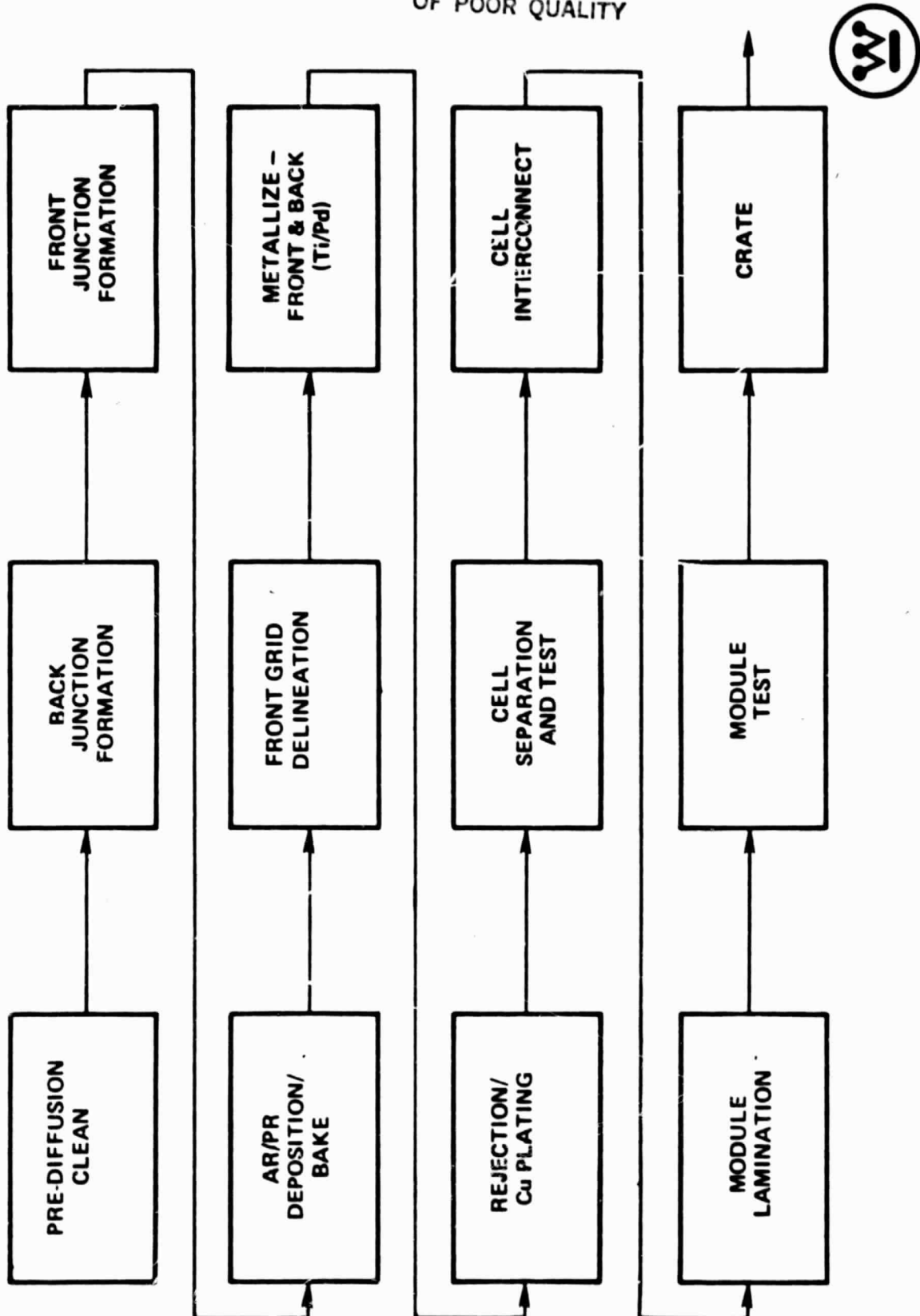


Figure 16. Westinghouse MEPSDU Overall Process Sequence

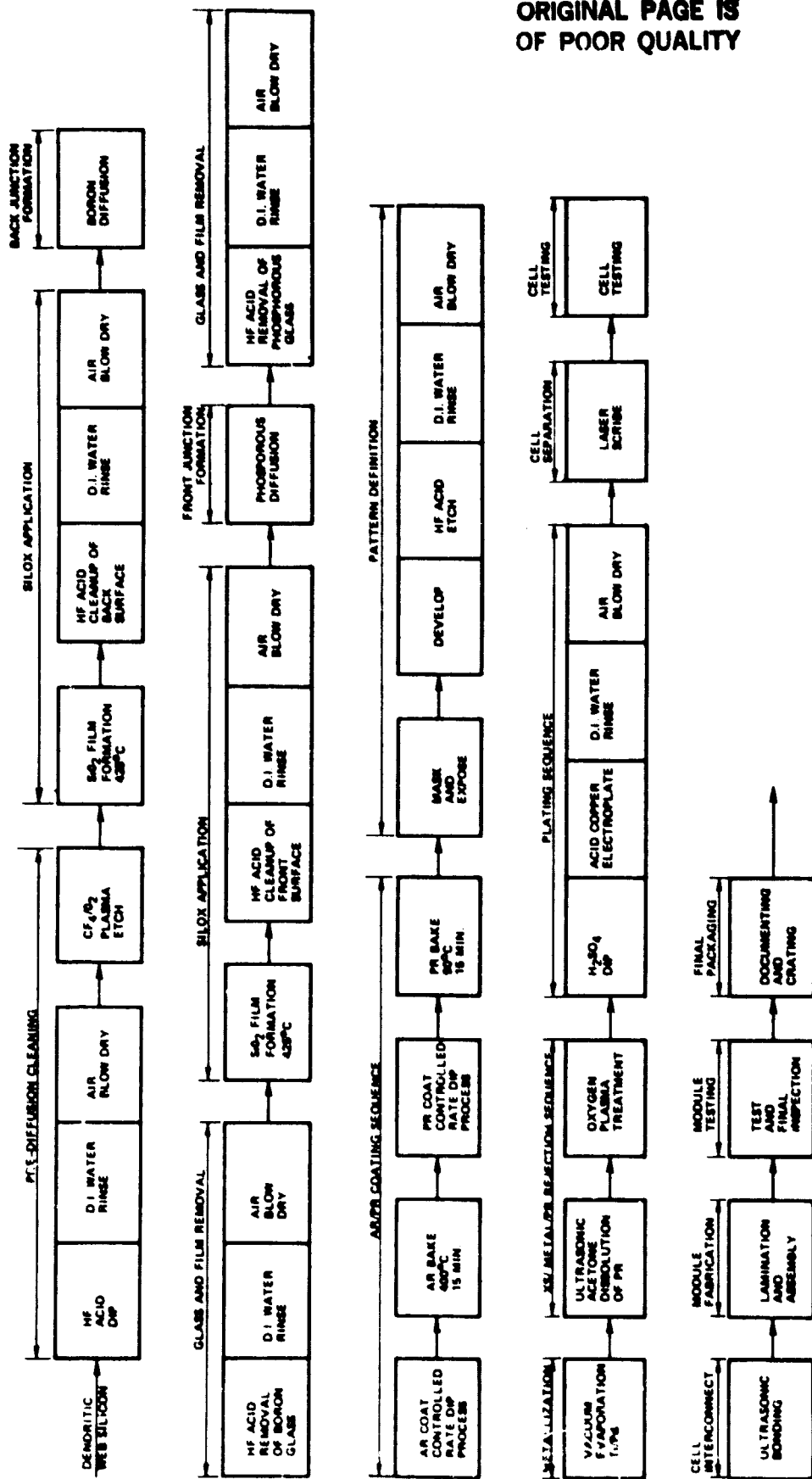


Figure 17. Westinghouse MEPSDU Baseline Process Sequence Flow Chart



repeated for the front surface where the junction is formed by phosphorous diffusion.

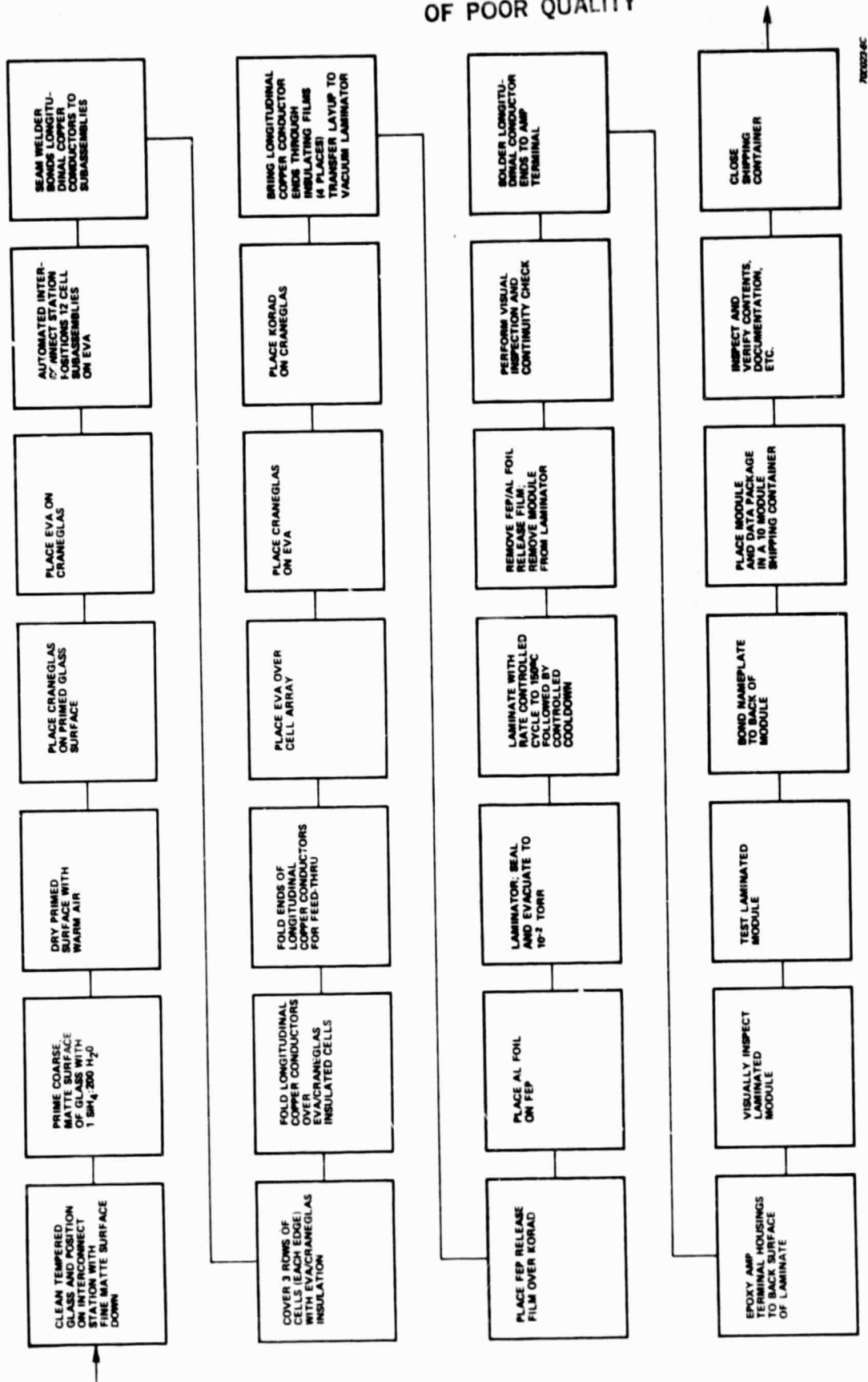
3. Antireflective (AR) and Photoresist (PR) Coating Application - The AR coating is applied first by controlled rate withdrawal from an organo-metallic solution to give a liquid film that is converted to  $TiO_2/SiO_2$  after baking. The PR coating is then applied, and its thickness is controlled in a similar manner.
4. Grid Pattern Definition - Standard photolithographic techniques of masking, exposing, developing, and pattern etching are employed.
5. Metallization - Successive layers of Ti and Pd are deposited on the web by vacuum deposition.
6. Metal Rejection and Plating - Excess metal and photoresist are removed by ultrasonic dissolution of the PR in acetone. Residual PR is removed by plasma stripping. Copper is electroplated over the vacuum deposited metal film.
7. Cell Separation - Four cells are separated from the 42 cm web strip using a laser scribe followed by a mechanical breakout.
8. Cell Test - The I-V characteristic of each cell is measured at AM1,  $100 \text{ mW/cm}^2$  and  $25^\circ\text{C}$ .
9. Cell Interconnection - Strings of 15 cells are electrically joined in series with aluminum interconnects by ultrasonic bonding.
10. Module Lamination - Modules are built from 12 parallel connected strings of cells using a layup process of glass and polymeric materials that are laminated into a module.

11. **Module Test** - The I-V characteristic of each module is measured at AM1,  $100 \text{ mW/cm}^2$  and  $25^\circ\text{C}$  cell temperature.
12. **Module Package** - Acceptable modules are crated for shipping.

The detailed steps required for Items 10, 11, and 12 are shown in Figure 18. This figure is a manufacturing flow chart of the module assembly operations. The sequence is as follows:

1. **Superstrate Preparation** - Low iron, tempered drawn glass of the proper size is cleaned with a commercial glass cleaner and positioned with the fine matte surface down. (The fine matte surface will be the sun side of the module.) The coarse matte surface of the opposite side is primed with a dilute solution of an organofunctional silane and dried with warm air.
2. **Layup Installation** - A spacer of Craneglas is placed on the primed glass surface. Ethylene vinyl acetate (EVA), used as a lamination pottant, is placed on the Craneglas. The sunside layup is then transferred to the string layup position of the automatic interconnect station.
3. **Positioning of Cell Subassemblies** - The cell stringing and tabbing machine uses an ultrasonic rolling spot bonder to form a series string of 15 interconnected cells. Twelve of these series strings are sequentially and automatically positioned by the automated tabbing and stringing machine on the EVA of the sunside layup. This subassembly is then moved to a finish layup station.
4. **Installation of Longitudinal Conductors** - The end interconnect tabs from each of the twelve series strings are ultrasonically seam welded to longitudinal copper conductors. Three rows of cells on each edge of the strings are covered with EVA/Craneglas to insulate the cells from the longitudinal conductors as they are folded back over the cells and brought into a position where the ends of the conductors can be brought through the dark side layup.

ORIGINAL PAGE IS  
OF POOR QUALITY



REC02046C

Figure 18. Westinghouse MEPDSU Module Assembly Flow Chart

5. Dark Side Layup Installation - A layer of EVA pottant is placed over the cell array. This is followed by the positioning of a layer of Craneglas and installation of the back cover film of Korad. The ends of the copper longitudinal conductors are brought through each of these insulating films as they are placed in position. The final layup is transferred (sunside down) to the vacuum laminator.
6. Lamination - Release films of aluminum foil and fluorinated ethylene propylene copolymer (FEP) are placed over the module layup, and the module is moved to the vacuum bag laminator. This laminator consists of two separate compartments which can be individually evacuated or pressurized. These compartments are separated by a flexible rubber diaphragm. With the module in the lower compartment, the laminator is sealed, both compartments are evacuated to  $10^{-2}$  torr, and the temperature raised to  $110^{\circ}\text{C}$  in less than 30 minutes. At this point, the upper compartment of the laminator is vented to atmospheric pressure which forces the rubber diaphragm over the module producing a uniform pressure. The temperature is raised to  $150^{\circ}\text{C}$ , and then the system is cooled to room temperature. The FEP/Al foil release films are removed, and a visual inspection and electrical continuity check performed.
7. Electrical Terminal Installation - Pre-tinned electrical terminal end conductors are soldered to the two bus bars. The back cover/end conductor penetrations are enclosed by a conductor housing that is attached to the back surface of the laminate using an epoxy adhesive formulated for this service.
8. Inspect and Test - A visual inspection of the assembled module is performed, and the current-voltage characteristics of each module are measured at AM1,  $100 \text{ mW/cm}^2$  and  $25^{\circ}\text{C}$ .
9. Nameplate Installation - A nameplate containing identification and electrical characteristics is attached to the back of the module.

10. Module Packaging - Acceptable modules are crated for shipping. Each shipping container holds ten modules and their respective data packages. The contents of each shipping container are verified, and the container is closed.

Verification of the adequacy of the Baseline Process Sequence was established during the course of the MEPSDU contract. This verification was achieved by:

1. Calculating all cost factors associated with each step of the process sequence and, using SAMICS methodology, determining that an overall production cost of 70¢/peak watt (1980\$ in 1986) was achievable in a large scale, fully automated production facility (see Section VII).
2. Fabricating mockups or full sized modules using the Baseline Process Sequence and testing to ensure compliance with environmental specifications contained in JPL Document 5101-138 (see Section III).
3. Fabricating a full size prototype module using the Baseline Process Sequence and testing to ensure that the 12 percent overall efficiency level used in the economic analysis could be achieved (see Section III).

#### B. Alternate Process Sequence Steps

During the course of the MEPSDU contract, several alternates to steps defined in the Baseline Process Sequence were evaluated in an attempt to demonstrate the potential for reducing processing or production costs below the level evaluated for the baseline sequence.

##### 1. Alternate Metallization Procedures

###### 1.1 Evaporated Systems

The initial baseline Westinghouse MESPDU process sequence specified a metallization system comprised of evaporated layers of Ti, Pd, and Ag followed by an electroplated layer of Cu. An in-house effort was directed toward the study of alternate metallization schemes which could improve the cost effectiveness of the baseline metallization system by reducing costs of the metals used or identifying less expensive equipment for applying the metals.

The first modification studied was the replacement of the evaporated layer of silver with copper. An evaporated Ti/Pd/Cu plus electroplated Cu metallization system was presented as part of the initial baseline process sequence at the Preliminary Design Review. At that time, the possibility of etching the evaporated copper to provide a fresh surface for electroplated copper (with the intent of eliminating the need for plasma ashing equipment) was under consideration. In reviewing the evaporated Ti/Pd/Cu process, it was noted that contamination of the titanium and palladium targets could occur during the vacuum evaporation of copper and that eliminating this possibility by depositing copper in a separate chamber was not cost effective. Therefore, a test was made to change the baseline metallization system to evaporated Ti/Pd, plasma ashing, electroplated copper. Experiments verified that this system, comprised of 500 Å Ti, 500 Å Pd, and about 8 microns of copper had excellent adherence on both the front (grid) and back surfaces and was incorporated into the MEPSDU baseline metallization system.

## 1.2 Non-Evaporative Metallization Systems

Scoping work on several significantly modified metallization systems to the baseline evaporated Ti/Pd/Plated Cu process was also performed on the MEPSDU contract. This scoping work narrowed the number of systems that were given experimental follow-up to two: (1) electroless nickel deposition on evaporated titanium, and (2) electroless nickel deposition on silicon after proper activation of the surface. In the Westinghouse MEPSDU sequence, particular attention must be given to the effect of aggressive etching or activating solutions upon not only the shallow junctions but also upon the AR and PR coatings which are applied before metallization. This is of greatest concern in the deposition of electroless nickel directly on silicon. Two vendors assisted in these follow-up experiments.

In the first case, that of electroless nickel deposition on evaporated titanium, the etchants employed by the vendor were too aggressive and etched through the evaporated titanium film. This approach was abandoned. In the second case, that of electroless nickel deposition on silicon in the presence of AR and PR

coatings, both vendors cited attack of the PR coating in the heated (approximately 90°C) electroless nickel baths. (Both vendors were working with silicon web that was supplied to them by Westinghouse after AR/PR coating, pattern exposure, development, and oxide etching. The PR coating had received the standard soft bake for 15-20 minutes at 90°C.)

Subsequent work continued with one of the vendors on the deposition of electroless nickel on silicon. Investigations included: (1) deposition of electroless nickel on a patterned sample given a post-bake treatment to improve the chemical and heat resistance of the PR coating, and (2) deposition of electroless nickel on silicon followed by the use of a negative resist.

A proprietary, highly alkaline nickel activating solution that showed promise on bare silicon was found to be too sensitive to deposition conditions to be used as a production process. Because the solution was highly alkaline, it also attacked the post-baked positive PR coating and, therefore, could not be used on partially processed samples. Additional work by the vendor yielded a new process that was claimed to be very reproducible with very few voids and with improved adhesion to silicon.

Using this process, numerous in-house experiments were conducted. In all cases, the inability to deposit a continuous, adherent nickel film on the web in a minimum number of process steps has made this approach less attractive than the reliable evaporation process identified in the baseline sequence. These results, in conjunction with results of a separate DOE/JPL sponsored program (Contract No. 955624) conducted recently at the Westinghouse R&D Center which suggest that nickel is not an effective long-term diffusion barrier for copper, led to abandoning the use of electroless nickel on the Westinghouse MEPSDU.

## 2. Dry Processing Experiments

An investigation into the use of dry plasma processing was carried out to replace many of the wet chemistry steps identified in the baseline process sequence. These steps include oxide removal from as-grown web, pre-diffusion

cleaning, and surface clean up prior to metallization and plating. In the plasma etch operation, the active species formed by an rf glow discharge react with impurities on the silicon surface and are removed as volatile products that are pumped from the system. The as-grown web has a coating of both a loose and an adherent oxide which must be removed before the first pre-diffusion cleaning. Therefore, these studies were concerned with both the standard pre-diffusion cleaning and oxide removal plus pre-diffusion cleaning.

Scoping experiments using raw web indicated that an agitated HF dip is inadequate in removing both loose and adherent oxide. However, both types of oxides are removed by lightly rubbing the surface with an HF saturated swab prior to plasma etching. Samples which had the best plasma etched appearance were processed in standard 96%  $\text{CF}_4$ :4%  $\text{O}_2$  etching gas for 2 min. at 300 watts or 10 min. at 100 watts. Those processed for longer times or at higher powers exhibited roughening of the surface.

A test was made in which three sets of samples were pre-diffusion cleaned as follows:

- Group I - Web wiped with cotton swab and plasma etched.
- Group II - Web wiped with HF/ $\text{H}_2\text{O}$  and plasma etched.
- Group III - Web given standard semiconductor pre-diffusion cleaning.

These groups, containing a total of 32 cells, were then processed together through the Westinghouse Pre-Pilot Facility. The standard baseline process was used for all other operations.

Web from Group I (dry wiped with a cotton swab to remove loose oxide) had, in many cases, a post-plating copper haze and yielded cells of poorer quality than did web swabbed with the acid solution. In general, cells produced from web given an acid swab and a plasma etch were equal to those produced from web given the standard semiconductor pre-diffusion cleaning process, which verifies the selection of the plasma technique in the Baseline Process Sequence.



Screening tests were performed by a vendor to establish conditions for cleaning raw web by plasma processing. Their findings were similar in that using the standard 96/4:CF<sub>4</sub>/O<sub>2</sub> etching gas without prior oxide removal, the silicon surface is not uniformly etched. Table 11 summarizes their results.

After 50 min. of etching with a 30/70:CF<sub>4</sub>/O<sub>2</sub> plasma at 85 watts R.F. power, there was no SiO<sub>2</sub> powder present; and, although there was a suggestion of a nonuniform adherent oxide, the surface had a reflectivity similar to web cleaned by standard wet chemical techniques. However, the time is considered excessive for cost effective processing; and, therefore, a combination of wet chemical/plasma etch processing was pursued.

Work on this task was then focused on developing a non-contact cleaning method to replace web scrubbing operations. Samples were sent out for vendor trials of cleaning in a "Megasonic" unit to determine if it will effectively remove oxide particles from the web surface in preparation for plasma etching. In these trials, a Megasonic cleaner modified (a vitreous carbon faceplate was substituted for the standard tantalum faceplate) for use with HF was filled with a solution of 1 part of HF in 10 parts of water and agitated. Samples of dendritic web with growth oxide on their surfaces were placed in the solution (equilibrium temperature of 45°C) for times up to 9 minutes. Samples processed in this manner were not completely free of loose oxide; however, there was an improvement with time. Thus, the need for longer immersion times, stronger solutions, or other solutions was indicated.

While arrangements were being made for follow-up trials, the vitreous carbon faceplate in the transducer array panel failed; and the vendor's original customer switched to an acid other than HF for his etching and, therefore, could use a standard Megasonic unit. Because of the high cost of preparing a new faceplate, the vendor decided not to repair the equipment without customer support. The cost of this repair to run additional trials without assured success was beyond the means of the MEPSDU contract; and, therefore, a new approach using a standard Megasonic cleaner and an altered sequence was currently under consideration at the time work was stopped on the MEPSDU contract.

TABLE 11

## PLASMA ETCHING OF RAW WEB

<u>Plasma</u>	<u>Pressure (torr)</u>	<u>R. F. Power (watts)</u>	<u>Time (min.)</u>	<u>Comments</u>
Argon	.4-.6	300-500	2-15	No reaction.
96/4:CF <sub>4</sub> /O <sub>2</sub>	.3	300	2-6	Non-uniform surface attack.
30/70:CF <sub>4</sub> /O <sub>2</sub>	.1-.3	85-400	1-50	Best results obtained at 85W and times in excess of 5 min.
5/95:CF <sub>4</sub> /O <sub>2</sub>	.3-.4	250-350	5-10	Surface clouding due to ex- cess oxidation.

At the present time, the baseline sequence incorporates an HF scrub for oxide removal before proceeding to the first pre-diffusion cleaning. Automated equipment is available for this scrubbing operation, and this equipment is being considered for the Westinghouse semi-automated production line. The experiments discussed previously, however, showed that an acid dip and plasma etch is a suitable, cost effective step for pre-diffusion cleaning.

### 3. Liquid Precursor Films for Diffusion Masks

The baseline process sequence specifies a chemical vapor deposited  $\text{SiO}_2$  film to be used as a diffusion mask prior to the two junction diffusion processes. This mask is required to allow diffusion in only one surface of the web (front or back) at a time. Although the formation of an  $\text{SiO}_2$  film from silane oxidation produces an effective diffusion mask on one side of the web, there is always some spotty deposition on the reverse side; and a quick acid dip is required to provide a clean surface for diffusion. A film from a liquid precursor, however, can be applied to one surface and, thus, eliminate the acid clean up.

In the initial experiment, the Westinghouse antireflective (AR) coating (a  $\text{TiO}_2$ - $\text{SiO}_2$  solution in alcohol) was used as a diffusion barrier. There were two groups of web used in the experiment with the antireflective coating: Group No. 1 used the standard  $\text{SiO}_2$  (Silox) masking before boron and phosphorous diffusion, and Group No. 2 had the Westinghouse antireflective coating solution painted on one side of the web before diffusion.

It was difficult to etch the antireflective coating from the web after diffusion, particularly after phosphorous diffusion. In order to process this group into cells, it was necessary to acid scrub to remove the coating; and this procedure gave cells that were slightly discolored.

Test data from the cells indicated that the antireflective coating does act as a diffusion mask in that the measured cell parameters from the two groups were the same. However, the etching behavior of the coating precludes its use in a production facility.

A second diffusion barrier experiment was then performed in which a modified Westinghouse AR coating was used as a diffusion barrier. This solution contained only an  $\text{SiO}_2$  precursor, and the film formed from this solution did not completely oxidize in the diffusion furnace. Therefore, in contrast to cells masked using the standard Silox process, the cells were contaminated with carbon and gave very poor results in the subsequent gaseous diffusion processing steps. This diffusion masking method shows promise, but more control over the initial coating material and application is required.

#### 4. Liquid Dopant Diffusant Studies

Gaseous diffusion of boron and phosphorous to form the solar cell back and front junctions respectively is specified for the MEPSDU Baseline Process Sequence. Since these diffusions must be done at significantly different temperatures ( $960^\circ\text{C}$  for boron,  $850^\circ\text{C}$  for phosphorous), the diffusion processes require separate furnaces, significant web handling, etc. Although gaseous diffusion produces high efficiency cells and has been shown to meet the JPL/DOE cost goals, an alternative technique using doped liquid precursors as diffusion sources was investigated.

Initial experiments were conducted using several commercial grade dopants having different concentrations. Web coated with these dopants was processed at different temperatures to determine if suitable sheet resistivities for the  $n^+$  and  $p^+$  surfaces could be obtained. The main emphasis in the initial phase of the study was placed on finding materials and concentrations which would yield the proper sheet resistivities\* when diffused at the same temperature for the same time period. This would allow simultaneous diffusion of the p-type and n-type dopant source in a single furnace. Based on results of these experiments, more extensive tests were made using a commercial liquid dopant which in the early experiment showed promise.

The tests were carried out as follows:

- a. Boron dopant applied to one side of web strip and baked at  $200^\circ\text{C}$ .
- b. Phosphorous dopant applied to opposite side of web strip and baked at  $200^\circ\text{C}$ .

\*The MEPSDU specifications for sheet resistivity are:

Boron doped  $p^+$ :  $40 \pm 10 \ \Omega/\square$   
Phosphorous doped  $n^+$ :  $60 \pm 10 \ \Omega/\square$

- c. Web strip heated in an 80% N<sub>2</sub> - 20% O<sub>2</sub> ambient at 900-960°C and then slow cooled to 700°C.
- d. Baseline Process Sequence used to finish processing strip into cells.

The first group of cells processed in this experiment had sheet resistivities which fell out of the given specification, with the p+ resistivity being 70-150  $\Omega/\square$  while the n+ resistivity was 25-35  $\Omega/\square$ .

The efficiency of the cells processed from these diffusion experiments was 10.4  $\pm$  0.6% with a maximum efficiency of 11.3%. The efficiency was generally inversely proportional to the p+ sheet resistivity.

Several subsequent tests were made using liquid dopants from different suppliers and having different dopant concentrations. Table 12 gives the results from several of these tests. The table shows that cells fabricated from the same web growth run using liquid dopants have consistently lower efficiencies as compared to those fabricated using the gaseous diffusion process of the Baseline MEPSDU Process Sequence. This lower efficiency is due in part to non-optimum n and p sheet resistivities (p+ sheet resistivity is high by 25-50% while n+ is low by 25%).

Another factor which became more obvious during these tests is the poor surface quality of many of the cells after diffusion. This surface problem leads to irregular coverage of the AR coating and poor Cu plating in subsequent processing steps. This surface effect is believed due to the technique used for applying the liquid dopant. In tests conducted to date, the dopant has been applied using a sponge-squeegee method. After diffusion and diffusion glass removal, streaky surface color irregularities are noted which are apparently related to the dopant application. These same irregularities are then noted after the AR coating and electroplating step.

To eliminate this surface condition, alternate techniques for liquid application to dendritic web were investigated. Both paint-on and spin application techniques were pursued. The results were again unsuccessful due to nonuniform coverage of the liquid. Finally, experiments were initiated in which the liquid precursor was applied using a meniscus coating\* application technique.

---

\*Commercial equipment using this coating method has been developed by Integrated Technologies, Acushnet, MA.

TABLE 12

COMPARISON OF CELLS PRODUCED USING THE BASELINE PROCESS  
(GASEOUS DIFFUSION) AND LIQUID DOPANTS

<u>No.</u>	<u>Web Growth Run</u> Ⓜ Designation	<u>Web Quality (Efficiency - %)</u>		<u><math>\eta_1/\eta_0</math></u>
		<u>Baseline Process</u> $\eta_0$	<u>Liquid Dopant</u> $\eta_1$	
1	6-100	---	12.1	---
2	4-81	12.6	8.2	.65
3	1-120	12.9	10.6	.82
4	4-82	13.8	7.1	.51
5	7-47	11.3	10.6	.94
6	5-102	13.9	10.9	.78

NOTES: 1. All cells - 2.0 cm x 9.8 cm.  
2. Tested at AM-1; 100 mW/cm<sup>2</sup>.

Figure 19 is a schematic drawing of the meniscus fluid coater. The fluid is applied to a porous applicator. The substrate (web) is drawn across the top of the fluid meniscus which forms at the top of the applicator. The thickness of the meniscus (dimension  $t$  in Figure 19) is greater than the radius of web dendrities, and the fluid is applied evenly on the surface of the web. The application experiments were performed by the meniscus coating equipment vendor. It is anticipated that this application technique can be used for liquid dopants, antireflective coatings, and photoresist coatings as well as diffusion masks.

Due to the potential high payoff advantages associated with liquid junction formation and liquid application techniques, this research work was selected by JPL for continuation beyond the stop work date of February 10, 1982. Thus, this report does not finalize efforts in this area.

ORIGINAL PAGE IS  
OF POOR QUALITY

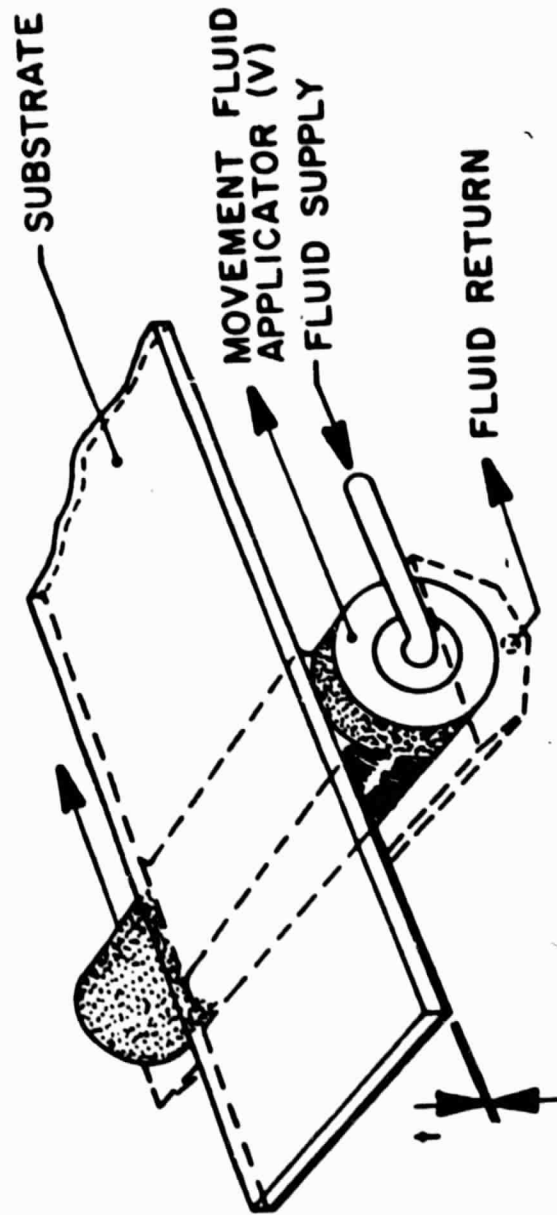


Figure 19. Meniscus Coating of Precursor Fluids to Dendritic Web Silicon



## VI. MEPSDU DESIGN

### A. General

As specified by the MEPSDU contract, demonstration of technical readiness of the Westinghouse photovoltaic module production process was to be achieved by designing or specifying and procuring all equipment required to fabricate modules using the specified process sequence. Primary engineering effort was focused on this phase (design and specification) at the time the stop work order was received from JPL on February 10, 1982. This section of the report summarizes the status of each Westinghouse MEPSDU process station as of that date.

In the case of equipment to be procured outside Westinghouse, purchasing specifications were prepared in accordance with Westinghouse Equipment Specification (E-Spec) procedures. The E-Specs are formal Westinghouse documents signed by appropriate Westinghouse management personnel, and the document follows rigorous configuration control procedures. Each E-Spec contains the following information:

1. Throughput of web required ( $200 \text{ cm}^2/\text{minute}$ )
2. Process requirements
3. Control requirements
4. Reproducibility requirements
5. Operation and maintenance manuals requirements
6. Preventative maintenance schedule
7. Recommended spare parts inventory
8. Installation and training requirements

### B. Pre-Diffusion Cleaning

The Baseline Westinghouse Process Sequence specifies a simple, efficient and cost effective process for pre-diffusion cleaning of dendritic web silicon. This two-step process consists of an acid dip followed by a plasma etch.

The etching station consists of a series of commercially available plastic tanks into which the dendritic web strips, mounted in plastic racks, are

immersed in HF and DI water for initial cleaning. After etching, the strips of web are unloaded from the plastic racks and placed in quartz boats for plasma cleaning.

As described in Section V of this report, substantial investigative work was underway to replace wet chemical cleaning operations of the baseline process sequence with dry processing operations at the time of the stop work order. Because of this effort, preparation of equipment specifications for this operation had not been initiated.

### C. Junction Formation Station

Gaseous diffusion of boron and phosphorous is used to form the back and front junctions respectively of the Westinghouse solar cells as specified in the MEPSDU baseline process sequence. The diffusions are carried out in a standard 5" diffusion tube furnace commercially available from numerous vendors.

An equipment specification was prepared for the diffusion furnace system required to perform front and back junction formations, as included in the baseline process sequence. Firm fixed price quotations were received from four vendors prior to receipt of the JPL stop work order.

In addition to the diffusion furnaces, a preliminary E-Spec was prepared for the CVD SiO<sub>2</sub> (Silox) reactor, which is required to deposit an SiO<sub>2</sub> diffusion barrier on the web strips prior to the diffusion step to prevent simultaneous front and back side diffusion. However, as discussed earlier in this report, it was hoped that this equipment would be replaced by a liquid meniscus coating apparatus; and vendor quotations to the E-Spec were not solicited.

After diffusion, an oxide etch is used to remove the phosphorous glass coating on the surface of the dendritic web strip. The web strips are removed from the quartz boats and placed in plastic racks similar to those used in the pre-diffusion cleaning operation. This station is the same as the first station in the pre-diffusion cleaning process and has the same throughput. Immersion of the diffused web into plastic tanks containing dilute HF and DI water

removes the boron or phosphorus glass that is formed on the web during diffusion. After the water rinse, the web is dried in a warm air stream.

#### D. Antireflective (AR) and Photoresist (PR) Application Stations

The Westinghouse MEPSDU baseline process sequence requires sequential application of two coatings to the surface of the dendritic web strips immediately after junction formation and removal of the diffusion oxides.

During the course of the program, an unsolicited proposal was received from a vendor for the design and fabrication of a device which will automatically dip a batch of web strips into the AR solution, withdraw the strips, hard bake the AR coatings, dip the batch of strips into the PR solution, and bake the PR coatings. The equipment would have the throughput capacity of the Westinghouse MEPSDU line and would require a single load and a single unload operation.

In the proposed system, two dipping tanks and two baking ovens would be used following techniques proven on the Westinghouse 50 kW Pre-Pilot Line facility. The four pieces of equipment (two tanks and two furnaces) are placed in a row with a support track overhead. The tanks are plastic, and the bake furnaces are commercially available, upright, open top furnaces.

The rate of withdrawal from the solution is controlled using a motor-driven screw mounted above the track which is moved along the tank. The motor has a reversible, wide range speed control for rapid motion or slower precision operation. Attached to the screw drive is a fixture, holding web lengths in a vertical position, much as a candle dipping procedure. The fixture will hold 60 pieces of web in a 10 x 6 matrix.

In operation, the web strips are fastened to the fixture, placed on the movable screw drive, and moved into position above the antireflection coating solution tank. A simple program logic controller processes the web through the four stations in the following sequence.

1. Rapidly dip dendritic web into the antireflection coating and remove at a controlled rate ( $\approx 2$  cm/min)

2. Horizontal translation of fixture above antireflection coating bake furnace
3. Rapidly lower web into bake furnace and hold (10 min)
4. Rapidly withdraw web from bake furnace
5. Horizontal translation of holding fixture to above photoresist tank
6. Rapidly lower web into photoresist coating and remove at a controlled rate (2 min)
7. Horizontal translation of fixture above photoresist bake furnace
8. Rapidly lower web into bake furnace and hold (14 min)
9. Remove from bake furnace and translate to end of line

The total processing time will be 28 minutes per fixture including translations, and the throughput rate exceeds the 2 web strip/minute (8 cells/min) throughput required for 1 MW/yr.

A second vendor initiated efforts to establish process parameters for applying AR and PR coatings in a meniscus coating system as described in Section V of this report. Conversations with the vendor indicate that progress was being made toward uniform coatings of the required thicknesses and that samples of coated material would soon be returned for evaluation. This coating technique is of interest because it can apply coating to only one side of the web and can be easily adapted to form part of an in-line processing system in the MEPSDU coat, bake, expose, develop, and etch sequence.

### E. Expose/Develop/Etch Station

Standard photolithographic techniques of masking, exposing, developing, and etching are used to define the electrical contact grid pattern on the front surface of the Westinghouse solar cell.

The station consists of exposure of the photoresist (PR) applied in the previous station, development of the exposed PR, and etching of the exposed antireflective (AR) coating. The process produces a grid pattern on the n<sup>+</sup> silicon of the front web surface and a clean p<sup>+</sup> back surface.

Since the baseline process for applying both the PR and AR is by dipping which coats both sides of the web strip, both sides of the web must be exposed, developed, and etched.

On the n<sup>+</sup> front surface, the PR is exposed through a contact mask which is a positive print of the grid structure. The p<sup>+</sup> back surface is totally exposed. During the development, the exposed PR is removed; and a grid pattern (down to the AR layer) is obtained on the front surface, and the AR on the back surface is exposed. The final step in the process is a mild HF etch which removes the AR from the back surface and from the grid pattern on the front surface. After rinsing and drying, the web strip is ready for metallization.

In the Westinghouse MEPSDU, a concept for the exposure system is being discussed with a vendor. In this preliminary design, 4-8 strips of 42 cm long web are loaded onto a fixture and held in place by vacuum. A hinged lid, containing the proper masks, is lowered over the web strips with the masks mating to the proper place on the web. An exposure lamp then traverses the web strips exposing the grid pattern. To expose the back, the strips are turned over and exposed without the masks.\*

---

\*As discussed in the previous section, application methods are presently being investigated where the PR and AR are applied only to the front surface. If this technique is satisfactory, exposure on the back will not be required.

The second piece of equipment for this station is a development and etching apparatus. For this process, a standard semiconductor processing station, modified to accept the long web lengths, will be used.

The web will be loaded into baskets and cycled through 5 substations: (1) developing solution, (2) DI H<sub>2</sub>O rinse, (3) etching solution, (4) DI H<sub>2</sub>O rinse, and (5) hot air drying station. The length of time at each substation will be controlled and programmed.

Several vendors of automated equipment performing all operations of the five identified substations have been contacted. In each, modifications would be required to accommodate the dimensions of the Westinghouse dendritic web strips. However, no problems are anticipated in engineering the machine to these specific requirements. In point of fact, nearly all units sold by the various vendors are modified to some extent.

E-Specs for the two pieces of equipment associated with the expose/develop/etch station were being prepared at the time of the JPL stop work order.

#### F. Metallization Box Coater

An E-Spec was prepared for the electron beam evaporation system required to perform base metal applications (Ti/Pd) as included in the baseline process sequence. The system would deposit these layers on both the front and back sides of the web. The machine needed for this station would be built from standard components (EB guns and power supplies, valves, pumps, thickness controllers, etc.) and engineered to the requirements of the E-Spec.

Highlights of the equipment requirements are summarized in Table 13. These requirements are well within commercial practice of large area, high throughput metallization system manufacturers. Commercial operating systems using electron beam evaporation have the capability of coating several hundred square meters per hour with a machine up time of greater than 90%.

TABLE 13

METALLIZATION BOX COATER SPECIFICATION HIGHLIGHTS

- Automatic operation
- Compartment deposition chamber with three evaporation stations (Temescal or equivalent SFIH-270-3 electron beam guns, 156 cc crucible capacity, single jacket)
- Diffusion pumped system (2-3 diffusion pump stations) with LN<sub>2</sub> traps or cryopumped system
- Process chamber at  $1 \times 10^{-6}$  torr or less during evaporation
- Film thickness control by EB gun power level and line speed (with quartz crystal monitors for initial set up and periodic checks)
- Full automation by relay logic or solid state (to be evaluated)
- Recommended spare parts inventory
- Vendor conducted training program on equipment operation and maintenance
- Detailed operating and maintenance manuals
- Optional conversion to planar magnetron sputtering by installing sputtering cathode, power supplies and argon backfill hardware

Firm fixed price quotations for the metallization box coater system had been received from five vendors prior to the JPL stop work order. Each of the proposed systems was responsive to the specification.

#### G. Metal Rejection/Plating Station

To insure minimum cost, the Westinghouse MEPSDU will carry out the rejection of the excess base metals applied to the front surface of the cells and the addition of copper plating to the grid lines and back side surface in a single unitized process station.

The rejection process uses acetone or other suitable solvent to dissolve the unexposed photoresist on the cell front surface, flushing away excess metal and leaving the grid delineated.

The use of such a plating station is well established. A similar (although larger) station is used by Westinghouse for plating battery grids. Its reliability has been established in over 10 years of routine, successful operation.

As noted in the cycle specification below, the MEPSDU rejection and plating station will consist of a series of 12 operations as shown in Table 14. Similar to the process station for antireflection coating and photoresist coating and baking, an overhead conveyor system will carry the web, loaded in racks, through the various tanks where a specific process will be performed.

A program logic controller will control the rate of progress of the web through the various tank stations with the program alterable at any time in the process. Thus, after the web is located on the fixture and the fixture enters the line, it will automatically progress to the end of the process step.

The dendritic web holding fixture will consist of a matrix of individual plastic holders with electrical connections to the web. Due to the high conductivity of the  $n^+$  diffused layer, contact can be made to any portion of the web where there is evaporated metal, e.g., on the dendrite outside the mask area. This eliminates tedious hand positioning of the electrical connection clips.



ORIGINAL PAGE IS  
OF POOR QUALITY

TABLE 14

REJECTION/PLATING STATION TREATMENT CYCLE

Operation Number	Description	Approximate Time
1	Load/Unload	7 Minutes
2	Acetone Bath	3 Minutes
3	Acetone Spray	1 Minute
4	Alcohol Spray	1 Minute
5 & 6	Deionized Water Rinse	Dip
7 & 8	Copper Plate	15-1/2 Minutes
9-10 & 11	Deionized Water Rinse	Dip
12	Hot Air Dry	7-1/2 Minutes

#### H. Cell Separation Station

In the Westinghouse MEPSDU process sequence, the separation of the four discrete solar cells from each dendrite-web matrix is accomplished by scribing the cell outline on the back of the web strip and fracturing out the individual cells. This scribing is accomplished using a Nd-YAG laser to penetrate into the back surface of the web strip about one third of its thickness.

An equipment specification for a laser scribe suitable for the MEPSDU throughput was prepared. Quotations were received from three vendors. A formal vendor selection was made, and a contract for this station was placed with Quantronix Corporation.

The laser scribe system described in the equipment specification consists of the following elements:

1. Nd-YAG laser powered by krypton arc lamps
2. Positioning fixture such that the web can be aligned to assure proper scribing directions and distances. This alignment is specified to be automatic - the operation constrained only to placing the web strip in a defined area. (This item is of prime importance in meeting the MEPSDU throughput requirement.)
3. A control unit which can be programmed to drive the fixture (or move the laser beam) through the required scribing path.

Figure 20 shows the layout of the automated laser scribe to be incorporated into the Westinghouse MEPSDU cell separation station. The system consists of a control unit, a power supply, and an opto-mechanical unit.

Table 15 lists the novel features of the Quantronix laser scribe. The most significant item in meeting the MEPSDU throughput requirements is the automatic alignment system, the key features of which are itemized in Table 16.

ORIGINAL PAGE IS  
OF POOR QUALITY

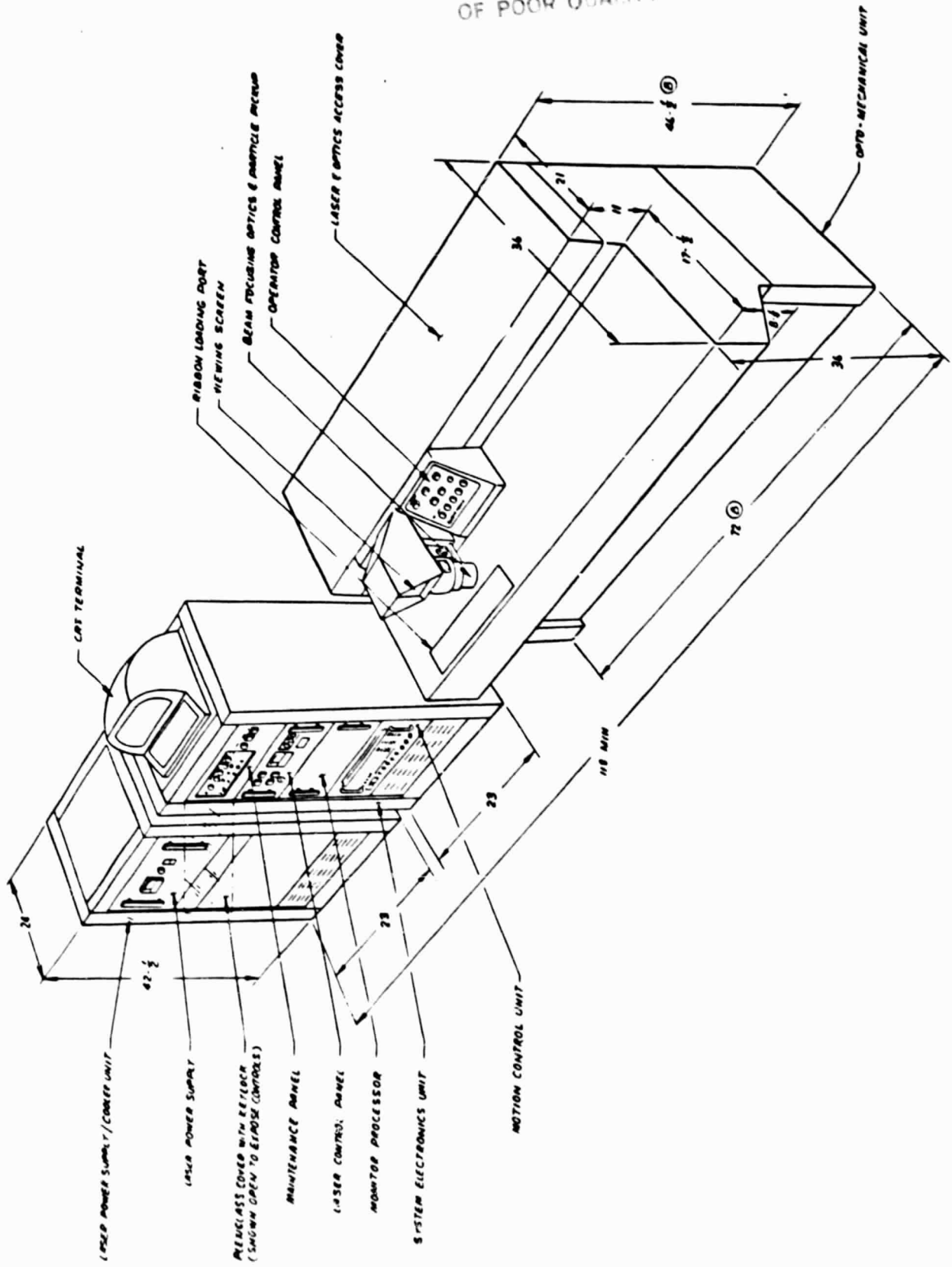


Figure 20. Automated Laser Scribe

TABLE 15

NOVEL FEATURES OF THE WESTINGHOUSE MEPSDU FACILITY LASER SCRIBE

- \* AUTOMATIC ALIGNMENT DETERMINATION INVOLVING STRIP POSITION MEASUREMENT AND SCRIBE PATTERN TRANSFORMATION RATHER THAN PHYSICAL MOTION OF THE STRIP ("INERTIALESS CORRECTION").
- \* A LARGE X-Y MOTION SYSTEM CAPABLE OF MOVING AN ENTIRE FIELD OF POSSIBLE STRIPS UNDER THE LASER BEAM.
- \* A VERSATILE TERMINAL DATA INPUT SYSTEM TO ALLOW FLEXIBILITY.
- \* SIMPLIFIED OPERATOR CONTROL AND EASY LOAD/UNLOAD ACCESS.
- \* NO EXTERNAL FIXTURES OR STRIP PREPARATION REQUIRED DURING LOAD/UNLOAD CYCLE.

TABLE 16

MEPSDU LASER SCRIBE AUTOMATIC ALIGNMENT SYSTEM FEATURES

- HIGH SPEED ACQUISITION OF COORDINATES OF FIDUCIAL MARKS ON CELL BY MEANS OF TABLE MOTION SCAN IN CONJUNCTION WITH CCD LINE SCAN CAMERA.
- HARDWARE PATTERN RECOGNITION OF CENTROID OF FIDUCIAL MARKS IN CROSS-SCAN AXIS BY DIGITAL TEMPLATE MATCHING.
- ACQUISITION OF CENTROID OF FIDUCIAL MARKS IN ALONG-SCAN AXIS BY MICROPROCESSOR CONTROL.
- RELATIVE IMMUNITY TO SPURIOUS SIGNALS DUE TO SPATIAL DISCRIMINATION ALONG TWO AXES.
- DISCRIMINATORS DESIGNED TO TOLERATE ELECTRONIC DROPOUTS DURING DATA ACQUISITION.

Table 17 presents time budgets for each phase of the laser scribe operation. With these time budgets, each strip of web material will be scribed into 4 cells in only 25 seconds. Thus, operating the system 22 hours per day, 340 days per year will produce the required cells for 1 MW production each year.

A Preliminary Design Review of the automated laser scribe was presented by the vendor, Quantronix, during December 1981. The design review was held at Westinghouse AESD and required a full day. Items presented and discussed were: the mechanical system description, arrangement (floor layout) drawings, motion system drive, microprocessor control, alignment pattern, utilities and installation requirements, control software, system flow charts, and operating sequence. Delivery of the unit is scheduled for September 1982.

#### I. Cell/Module Test Stations

Both the solar cell and module test stations for the Westinghouse MEPSDU were placed on order. The order consists of a M.A.P.S.S. solar simulator (medium area light source) and a semi-automatic cell test system with a digital electronic load to be interfaced with the M.A.P.S.S. data system. Both units are commercially available items manufactured by Spectrolab. Since the MEPSDU line will require testing a cell every five seconds and a module every half hour, it has been rationalized that a single data acquisition system can be utilized to interface with both a small area and large area light source and their associated data channels.

The Spectrolab M.A.P.S.S. module test station was delivered in early January 1982. Installation of the light source and module test fixture has been completed. Initial problems in both the computer test program and the printer have been rectified by the vendor, and final checkout of the unit was completed in February.

TABLE 17

LASER SCRIBE TIME BUDGETS

MANUAL LOAD	3 SEC. MAXIMUM
AUTO ALIGNMENT	5 SEC. MAXIMUM
SCRIBING (NOMINAL PATTERN)	14 SEC. MAXIMUM
MANUAL UNLOAD	<u>3 SEC. MAXIMUM</u>
	25 SEC. MAXIMUM, WORST CASE

## VII. KULICKE AND SOFFA SUBCONTRACT

### A. General

Westinghouse selected Kulicke and Soffa (K&S) Industries, Inc., as its subcontractor for the design and development of M JSDU equipment dealing with the automation of interconnection and assembly of its dendritic web silicon solar cells into modules. This subcontract deals with design, development, testing, and operation of equipment, and preparation of instruction manuals for the automated interconnect station.

The solar cell electrical interconnect configuration to be utilized by the interconnect station will be thin (.0015") aluminum tabs connecting metallized pads located on the front surfaces of each cell with the metallized rear surface of the adjacent cell. A major innovation in the Westinghouse cell interconnect station is the ultrasonic bonding technology to be used to join aluminum tabs to metallized cell surfaces. A rolling spot bonding technique has been developed by K&S specifically for this application.

As described in Section III of this report, the Westinghouse module will incorporate 12 separate cell string assemblies. Each cell string assembly will contain 15 individual cells electrically connected in series. The 12-cell string assemblies will be positioned by the automated cell interconnect station equipment to form an array of 12 rows of 15 cells each, with nominal dimensions of 16 x 48 inches. The target machine cycle is 5 seconds/cell with a yield of 95% or better. The machine will also include substations for making subsequent parallel or bus bar electrical interconnections of the 12 individual cell string assemblies.

Figure 21 is a schematic of the automated cell interconnect station showing the individual mechanical subsystems. Details and status of the subsystems at the time of the stop work order are described in the following sections.



ORIGINAL PAGE IS  
OF POOR QUALITY

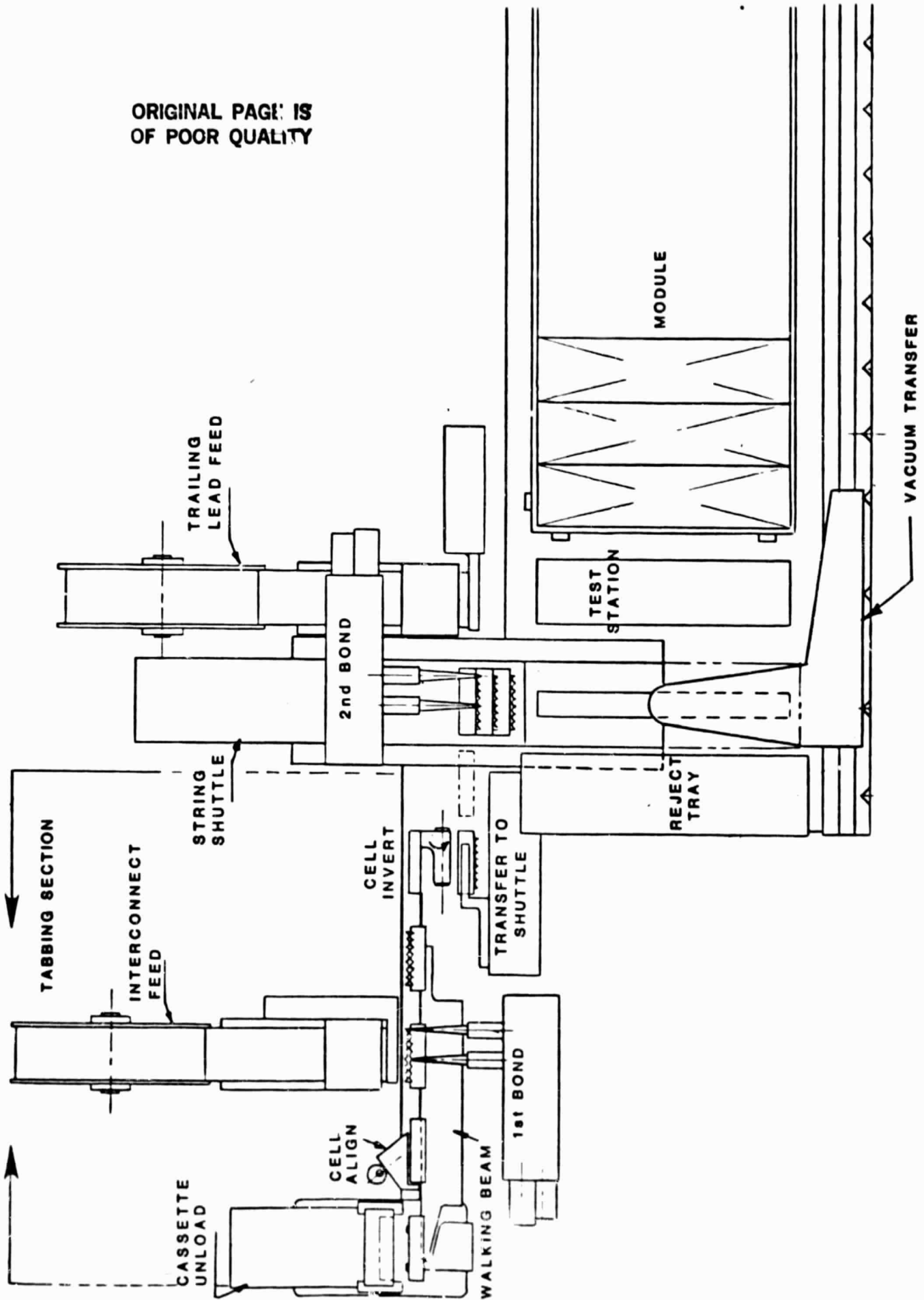


Figure 21. Westinghouse MEPSDU Automated Cell Interconnect Station

## B. Bonder

The heart of the automated cell interconnect station is the bonder. Ultrasonic joining techniques were selected to replace conventional reflow soldering for two primary reasons: first, the ultrasonic bond is performed more quickly allowing increased redundancy of interconnects (8 interconnect bonds are made on each cell), and second, no fluxes are required for the ultrasonic joining process eliminating the need for a post-bond cleanup operation.

During the initial phase of the Kulicke and Soffa subcontract, two ultrasonic bonding techniques were evaluated: rotary seam and rolling spot bonding. Actions of two types of ultrasonic bonders are shown in Figures 22 and 23. Satisfactory aluminum-to-cell bonds were achieved using both methods based on pull test strength and electrical resistance measurements. However, the rolling spot bonding technique was selected for use in the MEPSDU solar cell tabbing and stringing machine for the following reasons:

- Bond Cycle Time - To achieve the minimum throughput rate required with the seam bonding system, the seam roller would have to move from bond to bond at high speed. However, the relatively high mass of the seam roller, as compared to the spot bonding head, makes this high speed movement more difficult.
- Cell Efficiency - Basically, the seam bonding technique accomplishes bonding by a continual rolling motion of the bonding tool. Consequently, additional steps must be taken to prevent the tool from engaging the cell between bonds since this has a negative effect on cell efficiency. To ensure proper operation at the high speeds necessary to meet throughput requirements, this additional action would have to be accomplished in a manner that would also avoid excessive tool impact on the cell. The spot bonding tooling engages the cell only at the bond locations and, therefore, should not cause any decrease in cell efficiency.
- Multiple Heads - To achieve the required throughput with present equipment, it was found necessary to use two bonding heads. The

ORIGINAL PAGE IS  
OF POOR QUALITY

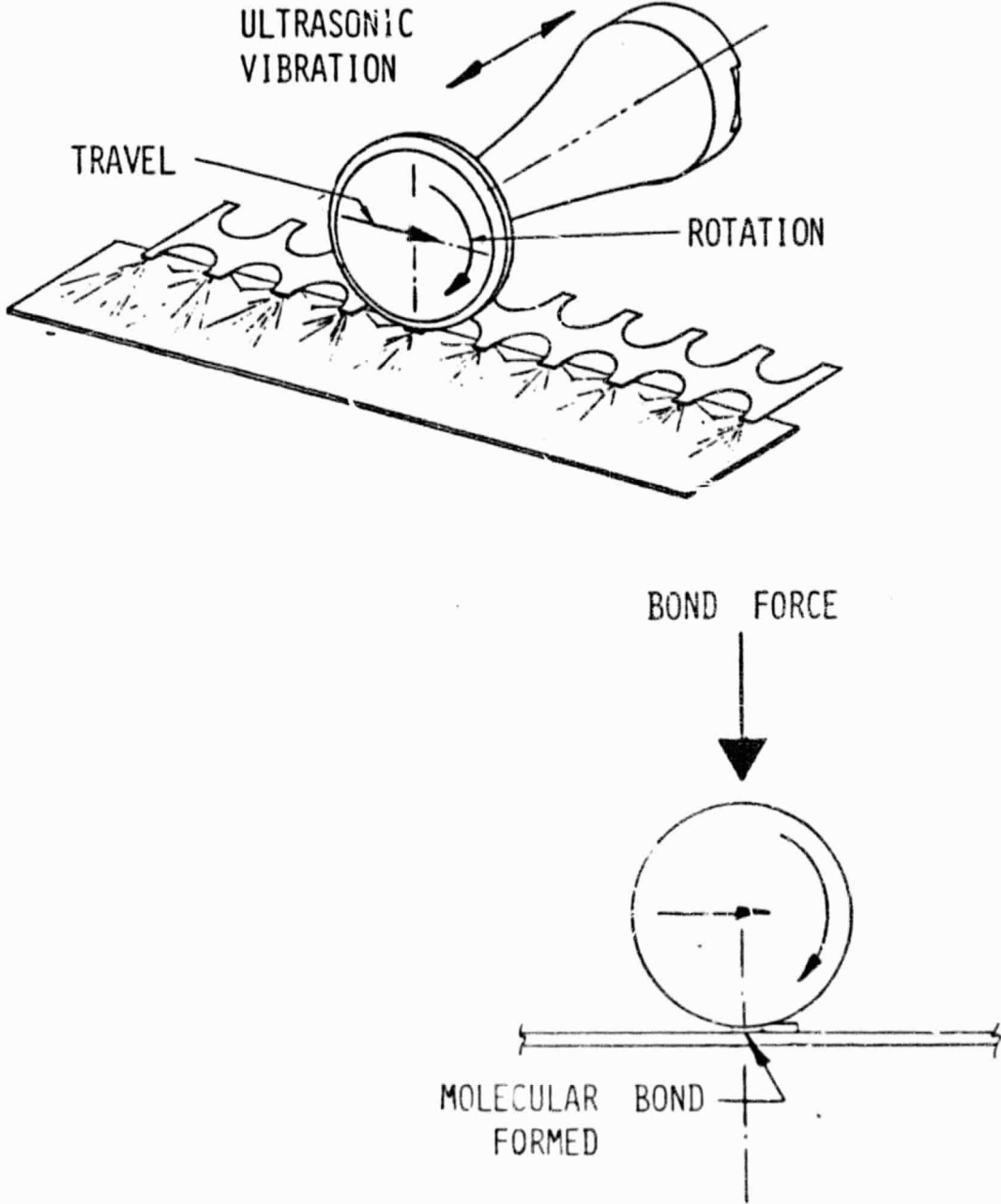


Figure 22. Rotary Ultrasonic Seam Bonding

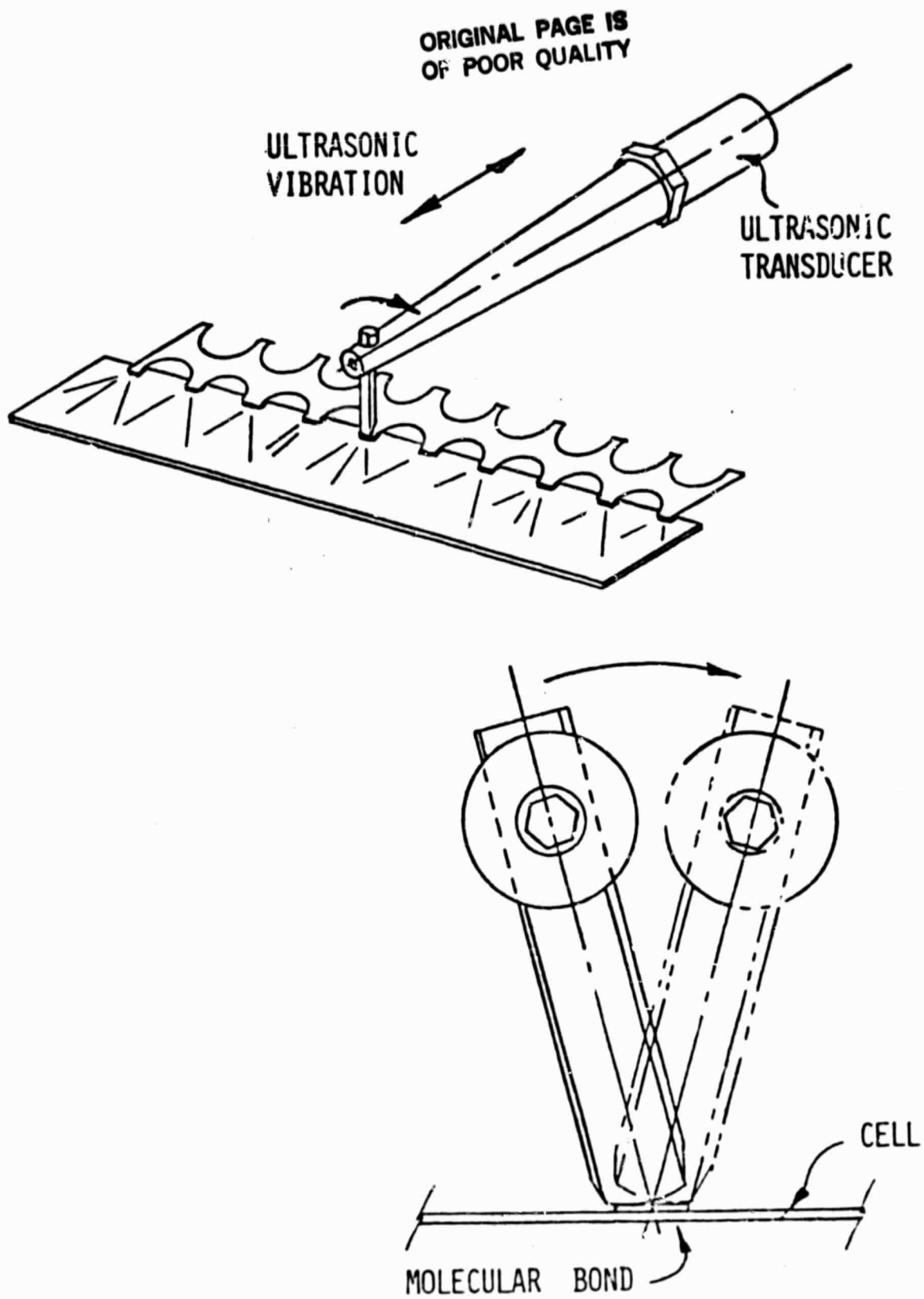


Figure 23. Rolling Spot Ultrasonic Bonding

lower mass of the spot bonding head permits the use of two parallel heads in the same bonding station. This would prove difficult with rotary seam bond tooling.

- Power Range - Present seam bonding equipment operates at the very low end of its capability which makes adjustment both more difficult and more critical. On the other hand, the spot bonding equipment operates at mid-range which is more stable.
- Bond Force - Spot bonding can be accomplished with less bond force than seam bonding. As a result, spot bonding subjects the solar cell to less localized stress which should result in less damage to cells.
- Tooling Flexibility - Tooling changes with the seam roller are limited and expensive since the entire horn must be changed. The spot bonding tools are simple carbide wedges which are inserted into the horn and may be changed easily. In addition, the carbide wedge wears longer than the hardened steel seam roller.
- Cost - The ultrasonic system and tooling required for the seam roller cost approximately ten times more than the ultrasonic generator, transducer, and wedge used for spot bonding.

After completing experimental work leading to the selection of the basic bonding configuration to be used on the machine, work was directed toward the design and fabrication of the actual bonding mechanism to be used for the first bond station. This mechanism is shown in Figure 24. As can be seen, the unit contains two heads: the first performs the bonds on cell pads 1 through 4 while the second head simultaneously bonds pads 5 through 8. Testing of this unit has demonstrated that electrical and mechanical bonds are satisfactory and that bond cycle time is under 2 seconds, which is approximately 30% lower than the budgeted time for this operation.

ORIGINAL PAGE IS  
OF POOR QUALITY

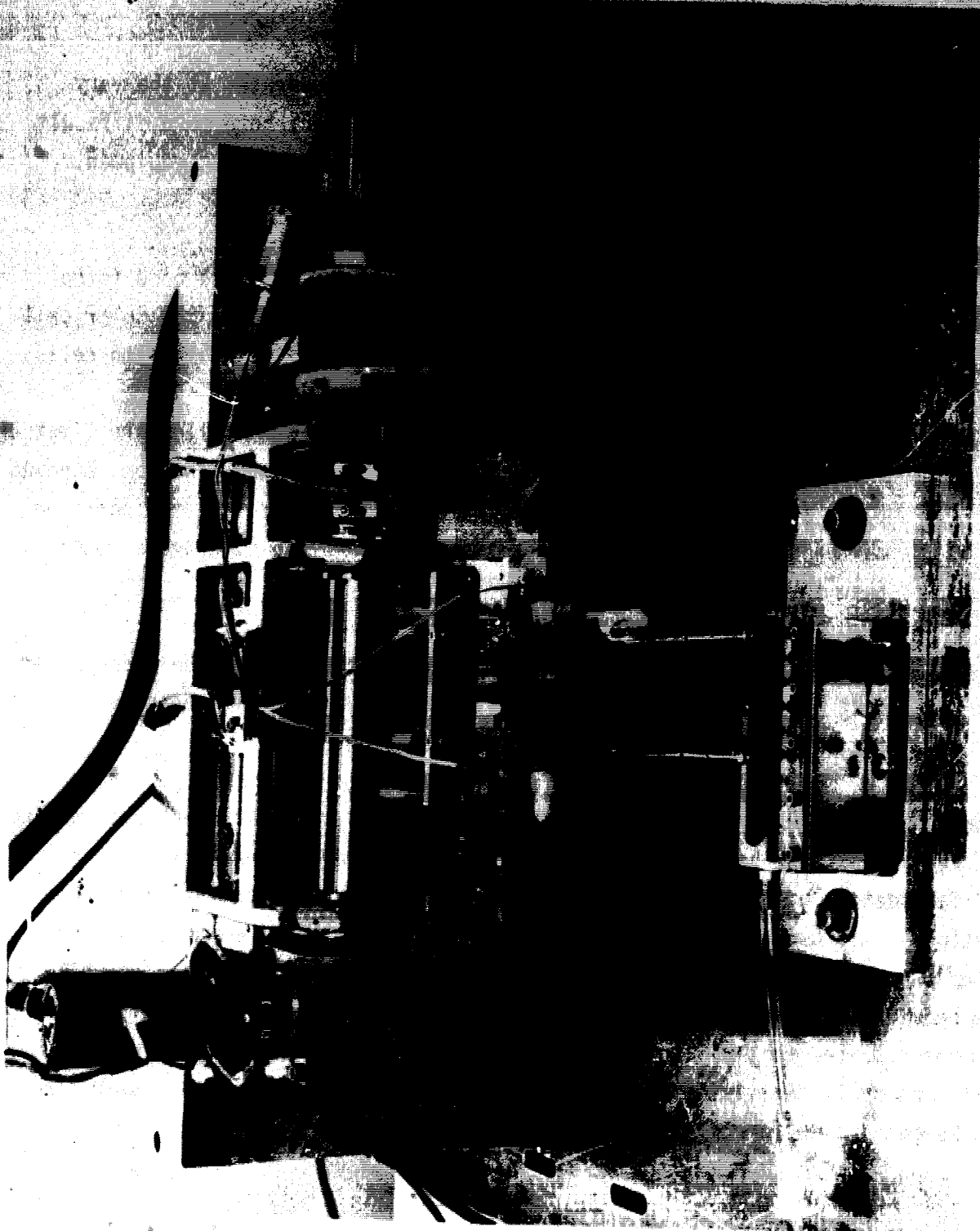


Figure 24. Bonding Mechanism for First Bond Station

C-2

### C. Cassette Unload Station

Operation of the automated cell interconnect station is initiated with the removal of a single cell from a preloaded cassette. The cassette is a "coin stack" configuration in which 25 individual cells are stacked one on top of another. The cassette is designed to prevent relative lateral motion of individual cells in order to eliminate potential surface damage.

Figure 25 is a photograph of a mockup cassette unload station built to test the concept. Cells are removed from the cassette using a dual vacuum cup pickup. An air jet is directed laterally on the stack of cells in the cassette to prevent them from sticking together during pickup operations. The cells are transported by the unload pickup device to the walking beam portion of the automated cell interconnect station (see Figure 2!).

After the cell is delivered to the walking beam, it is indexed to the alignment station and then to the first bond station.

### D. Bond Stations

In the first bond station, the aluminum interconnect is bonded to the pads on the front (sun) side of the cells. The interconnect is fed from a prepunched continuous roll of aluminum foil, sheared, and transferred into position over the cell, and bonded to the cell using the rolling spot bonding device discussed previously.

Figure 26 shows the interconnect feed mechanism loaded with the roll of .0015 inch thick prepunched aluminum foil. The shearing mechanism is shown in the photograph, but the interconnect transfer mechanism is not.

The walking beam conveyor then indexes the cell to an inverter system (refer to Figure 2!) which inverts the cell along with its attached interconnect and places it on the string conveyor in position for the extended interconnect to be bonded to the back of the previous cell. This bonding operation is performed with a two-head rolling spot bond device which is essentially identical to the

ORIGINAL PAGE IS  
OF POOR QUALITY

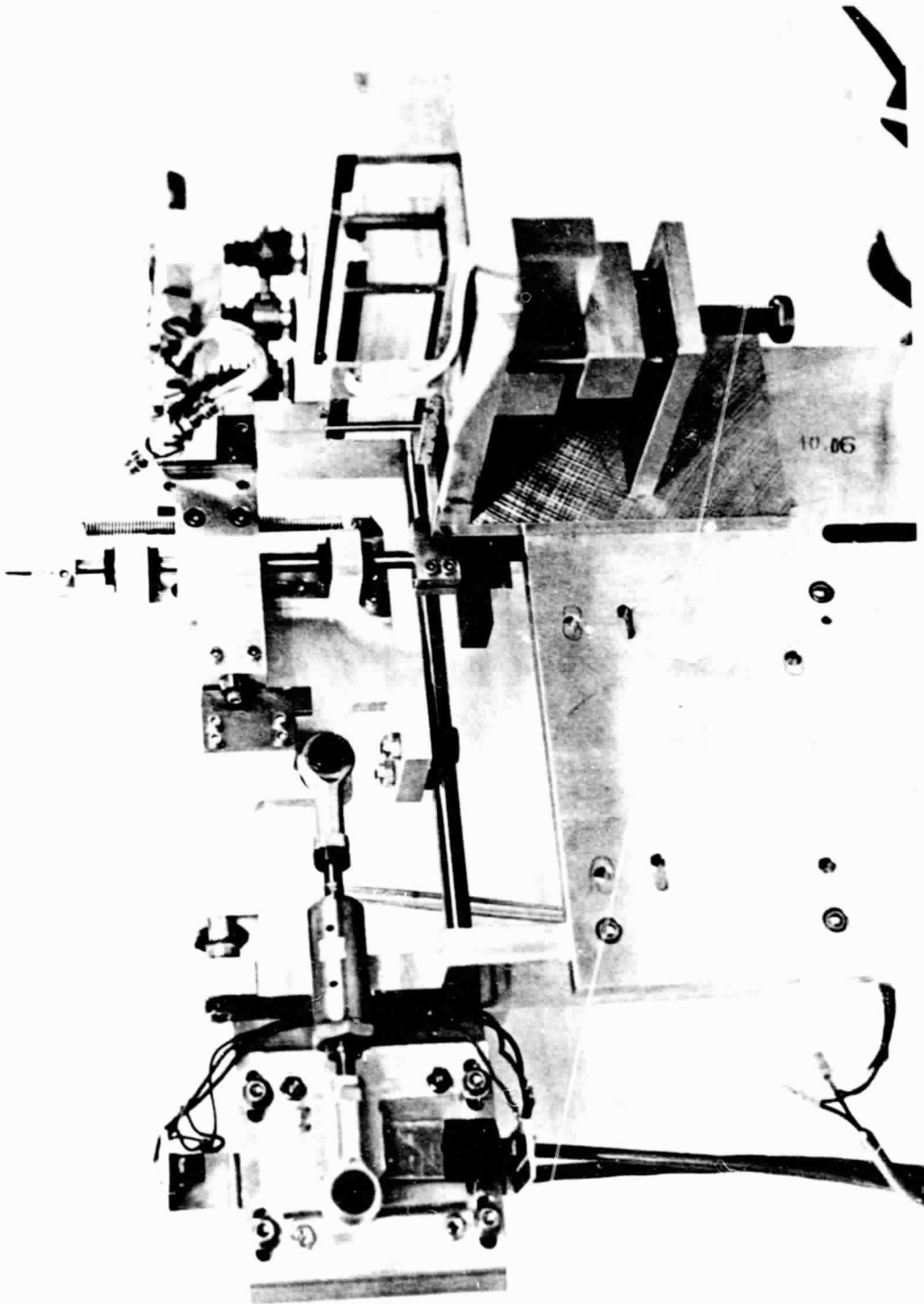


Figure 25. Mockup of Cassette Unload Station



ORIGINAL PAGE IS  
OF POOR QUALITY

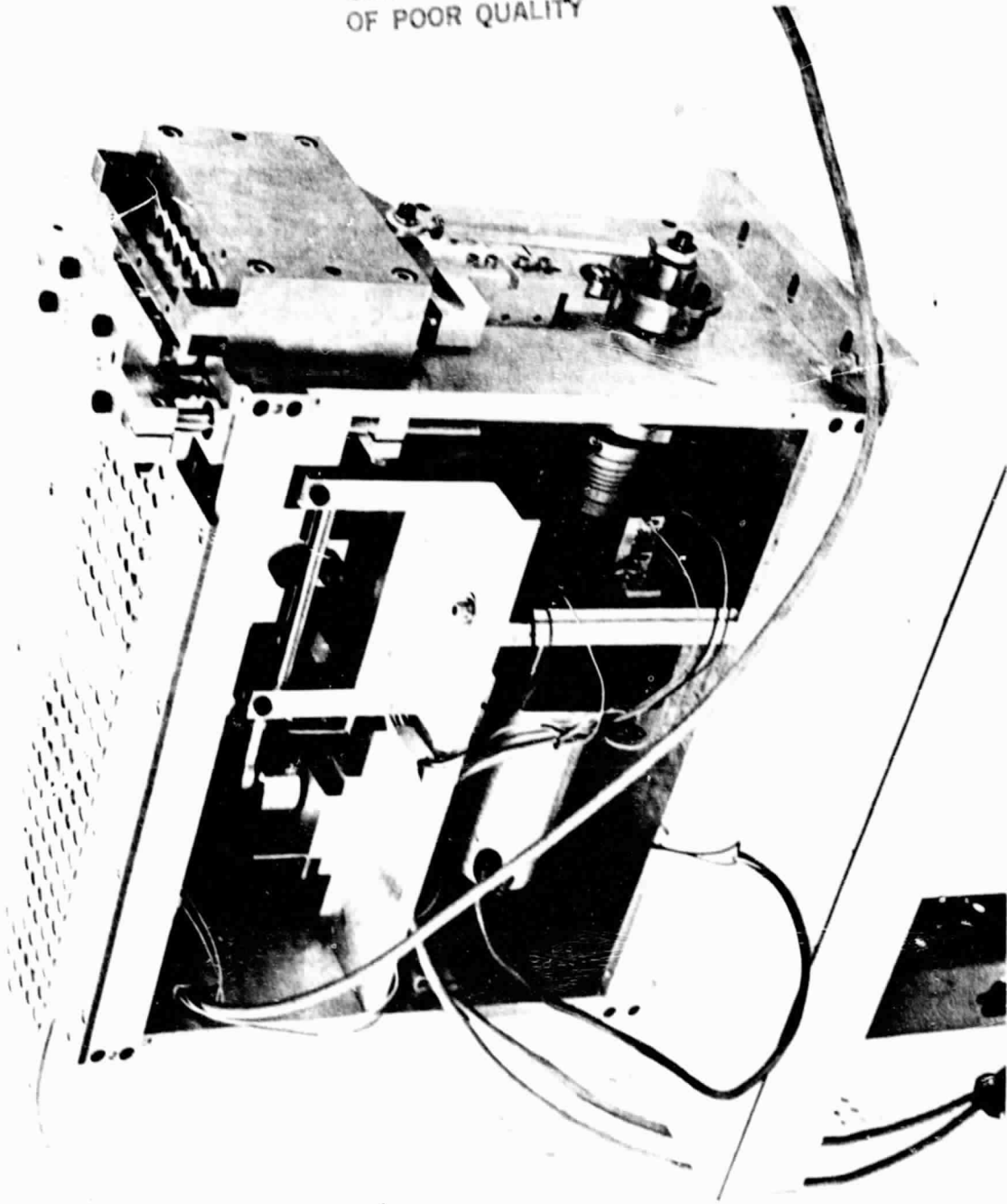


Figure 26. Interconnect Feed Station (Minus Ribbon Transfer Mechanism)

bonder used to make the front bonds. All bond parameters (i.e., force, speed, and excitation energy) are identical for the front and back bonds.

#### E. String Conveyor

A string conveyor is used to index cells as they are joined together into strings of fifteen cells approximately 16 inches in length (refer again to Figure 21).

A steel belt conveyor and a shuttle system were evaluated to determine the mechanism best suited for use as the cell string conveyor. The belt conveyor uses two parallel steel belts driven by sprocketed pulleys. The belts index continuously. Cells are transferred to the conveyor onto precise "pockets" defined by registration/retaining hardware on the belts. The pockets maintain the accuracy of intercell pitch (distance between cells).

The shuttle uses a reciprocating table, or plate, driven by a lead screw. The length of the plate corresponds to the length of the cell string to be made. The plate begins in a reset position at the cell transfer area and indexes (advances) one intercell pitch as each cell is deposited on the plate. After the complete string is formed, the plate indexes to the string pickup area, where the string is transferred to the module array area. The shuttle then returns to its reset position. The return to reset is an additional motion not required by the belt conveyor. However, the shuttle recovers this lost time by requiring less time for each index cycle. Cells can also be transferred to the shuttle faster because it uses no pockets, eliminating the additional care and time required to transfer a cell to such precise locations. The shuttle's reliability depends on the accuracy of cell transfer and elimination of any movement of the plate in relation to the cells during index cycles.

Based on the following factors, the shuttle was chosen as the system to be used for the string conveyor.

1. Handling and transfer of the cell to the shuttle presents fewer problems, minimizing the chance for cell breakage.

2. The shuttle's design allows optimizing intercell pitch to accommodate manufacturing tolerances. Index pitch is a programmable function and may be changed with minimal changing of parts.
3. The shuttle is a relatively simple mechanism, containing few parts, and should be less expensive.

When each string is completed, it is automatically picked up using a track-mounted vacuum lance and moved to a test station where the string will be electrically tested prior to being placed in the module array area in the format specified by the MEPSDU module assembly drawing. The vacuum lance maintains the intercell mechanical spacing, and a track will be provided with detents to locate the strings for correct interstring spacing. A reject station is provided in the discharge area in case it is determined that the cell string should not be delivered to the module array area.

#### F. Control System

An extensive survey was conducted to identify the optimum machine control system to be used for the automated cell interconnect station. The control system to be utilized is a programmable controller that is compatible with, and can be enhanced by, microprocessor and servo circuitry. A programmable controller is required to provide the flexibility desired in such equipment along with relative simplicity in programming, operation, and maintenance.

The following factors were considered in the evaluation of commercially available programmable controllers:

- Memory - Type and back-up
- Scan time (per 1K of memory)
- Types of input/output (I/O) interface available
- Programming features
- Service availability
- Manufacturer experience
- Price - based on:
  - Basic processor
  - Minimum memory
  - 150 I/O capability

This evaluation resulted in the selection of a GE Model 600 unit which has the high technical specifications required for this application. The unit's high scan speed (1 msec/1 K) eliminates the additional software and associated hardware development that would be required to adapt previously available controllers. The PC works in conjunction with a programming terminal capable of providing ladder diagrams, simulation data, and diagnostic data on the terminal's CRT screen for development and troubleshooting purposes, which makes the unit more desirable from a user standpoint.

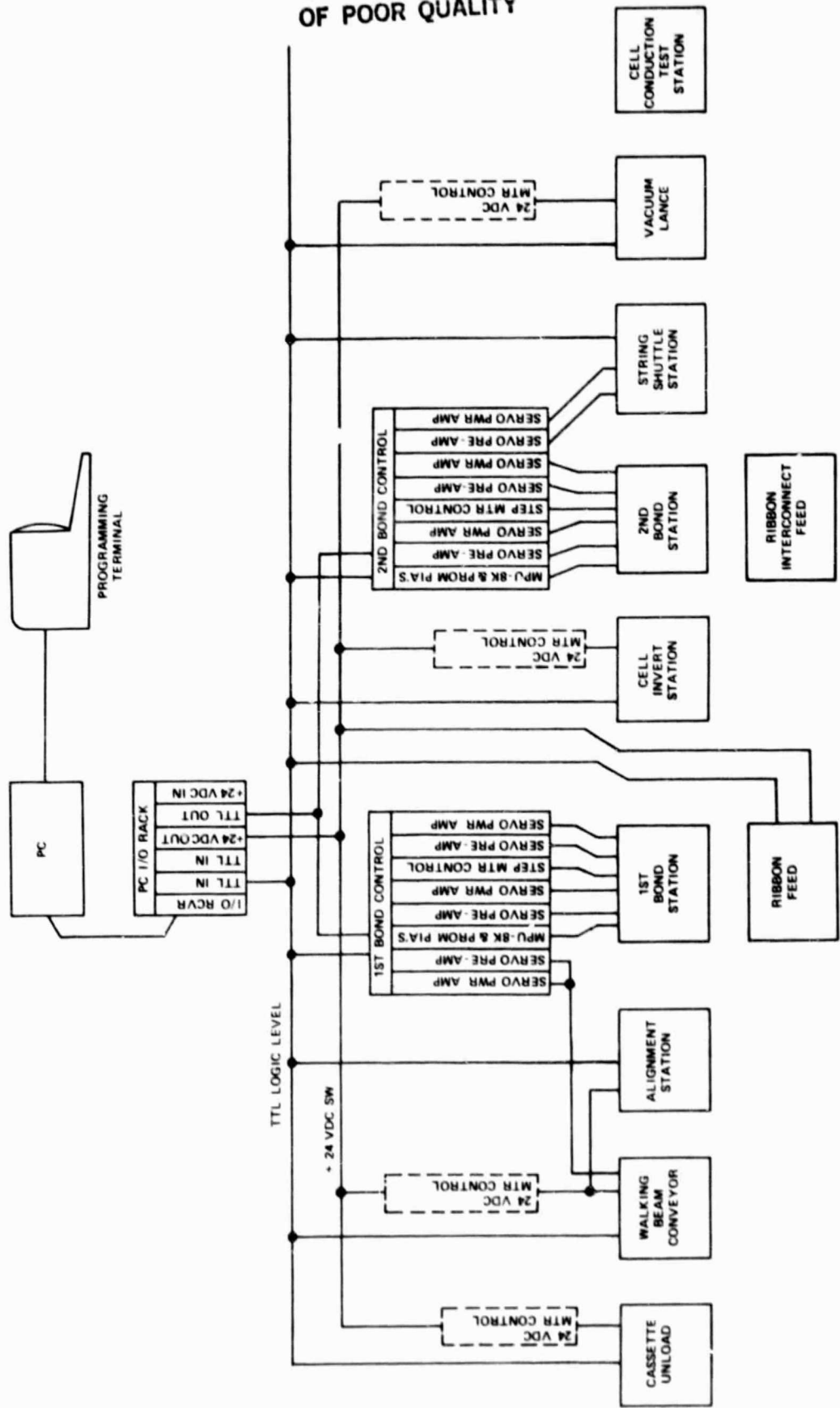
At the time of the JPL stop work order, work was proceeding on determining the complete machine sequence of events and developing timing diagrams to aid the programming effort. A block diagram of the control structure for first and second bond stations, including the PC and some microprocessor controls, is shown in Figure 27.

#### G. Design Review

A design review of the automated cell interconnect station was conducted at the K&S facility at Horsham, Pennsylvania, in November 1981. The Westinghouse design review team consisted of the MEPSDU Program Manager and two senior engineering personnel (one electrical and one mechanical) who are not directly related to the MEPSDU project. The primary purpose of the review was to establish that the equipment proposed by K&S could meet the requirements of the automated cell interconnect station equipment specification (E-Spec). This evaluation is necessary prior to placing the order for the Westinghouse funded equipment.

The evaluation team report was completed and indicated that K&S proposed equipment should meet the E-Spec requirements both electrically and mechanically. Accordingly, the Westinghouse capital equipment order was placed with K&S in January 1982. The design and fabrication effort continued under Westinghouse funding after receipt of the JPL stop work order received in February 1982.

ORIGINAL PAGE IS  
OF POOR QUALITY



706511-1A

Figure 27. Interconnect Station Control Structure

## VIII. ECONOMIC ANALYSES

### A. Background

During the course of the Westinghouse MEPSDU contract, a significant effort was completed to evaluate the cost of fabricating solar modules from dendritic web silicon using the Baseline Westinghouse Process Sequence. This economic analysis was conducted in iterative fashion in parallel with technical work on the contract. That is, as changes were made (or considered) to the baseline process sequence, the economic impact of these changes were evaluated.

To establish the capability for performing detailed in-house economic analyses, a computer terminal, including a CRT and Modem, was leased by Westinghouse and used exclusively for MEPSDU cost analysis (SAMICS). A Westinghouse engineer and a technician attended an introductory terminal usage seminar given by the computer leasing service personnel in Pittsburgh.

All economic analysis work required by the MEPSDU contract was performed. In all cost analysis SAMICS simulations, two separate production rates were assumed. The first production rate, 1 MW/yr, corresponds directly to the capacity of the Westinghouse MEPSDU facility. Then, to project high volume production costs, a similar analysis was made for an automated production facility having a 25 MW/yr production rate using the same process sequence. Throughout this report, these two simulations are referred to as the M-Process (1 MW/yr) and the P-Process (25 MW/yr).

To allow a direct comparison of costs of the individual steps within the process sequences, the 1 MW/yr and 25 MW/yr simulations follow the same sequence steps and use the same step referents.

Table 18 is a listing of the process steps and referents used for these two simulations. The eleven individual steps follow a natural grouping of sub-tasks within the process sequence.

The data used in the Format A's for the two processes were based on recent vendor quotes for capital equipment and materials. The material usage was based on calculated requirements and pre-pilot facility experience.

TABLE 18

## PROCESSES AND REFERENTS USED IN SAMICS COST ANALYSES

<u>Process #</u>	<u>Referent</u>	<u>Process Name</u>
M1/P1	CLENWEB	Pre-Diffusion Cleaning
M2/P2	DIFFWEB	Boron Diffusion
M3/P3	BSF	Phosphorous Diffusion
M4/P4	ARPR	Application of Antireflective Coating and Photoresist
M5/P5	GRIDDE	Expose, Develop, Etch
M6/P6	METWEB	Metallize
M7/P7	REJPL	Reject/Plating
M8/P8	TESCEL	Cell Separation and Test
M9/P9	INTCON	Cell Interconnection
M10/P10	LAMMOD	Module Lamination and Test
M11/P11	CRAMOD	Crating

## B. Assumptions Used in SAMICS Cost Analyses

- 3 shift, 345 days per year operation ( $4.97 \times 10^5$  operating minutes per year)
- The modules fabricated in both the 1 MW/yr M-Process and the 25 MW/yr P-Process facilities have nominal dimensions of 40 cm x 120 cm (16" x 48").
- These modules are assumed to produce 60 watts at 25°C and 100 mW/cm<sup>2</sup> insolation. This is based on module performance calculations presented in Section IV of this report.
- The M-Process assumes a throughput rate of 200 cm<sup>2</sup>/min of usable web ( $99.4 \times 10^2$  m<sup>2</sup>/yr).
- The P-Process assumes a throughput rate of 5000 cm<sup>2</sup>/min of usable web ( $2.485 \times 10^5$  m<sup>2</sup>/yr).
- The strips of dendritic web input into both processes are 42 cm long by 2.7 cm wide. From these strips four 2.5 cm x 10 cm (nominal) cells will be fabricated. The cost for the silicon used in the Format A input includes all losses due to non-utilization, e.g., dendrites and strip end losses.
- Yields for the process are taken into account in each step of the sequence. The assumed yields are based on projections from current yield data being observed in the Westinghouse Pre-Pilot Facility which operates using the Baseline Process Sequence.
- Machine up-time (A8 on Format A) assumed for each station is based on best industry experience.



- The maintenance and quality control personnel are included in costs associated with the specific process steps where they are required.
- Waste materials (organics, acids, oils, etc.) are disposed of by a local contractor. The Format A inputs for this disposal are derived from a vendor quote.
- Commodity and capital equipment costs are based on vendor estimates.
- In extrapolating from the 1 MW/yr M-Process to a 25 MW/yr P-Process, a highly automated factory was assumed. This automated factory concept increases capital cost but greatly decreases labor input. In general, the material usage was scaled very nearly proportional to the production rate with very small savings in usage assumed. This is a realistic assumption since most of the expensive materials (e.g., glass, laminating material, etc.) are area related and are absolutely proportional to production rate.

### C. Results and Conclusions

The first complete analysis was presented to JPL in topical report, which included SAMICS Format A's and a detailed description of the input data. This report was submitted to JPL in July 1981.

Subsequently, a workshop was held with JPL personnel to discuss the inputs and results of the first analysis and to identify modifications mutually agreed upon. The P-Process and M-Process analyses were then repeated, and results reported herein represent the final calculations.

Table 19 presents results of the SAMICS analysis of a 1 MW/yr (MEPSDU sized) production facility. Results are presented as the value added for each step in the Baseline Process Sequence. Also shown is the fraction of the total

TABLE 19

SAMICS COST ANALYSIS  
Value Added for Process Steps  
1 MW/yr Production Facility

<u>Process Step</u>	<u>Process</u>	<u>Value Added (1980\$/peak watt)</u>	<u>Percent of Total</u>
1	Prepare Input Web	0.615	18.9
2	Boron Diffusion	0.192	5.9
3	Phosphorous Diffusion	0.181	5.6
4	Application of AR/PR	0.182	5.6
5	Define Grid Pattern	0.193	5.9
6	Metallize Web	0.357	10.9
7	Rejection and Plating	0.307	9.4
8	Cell Separation and Test	0.576	17.7
9	Cell Interconnection	0.254	7.8
10	Lamination	0.345	10.6
11	Crating	0.061	1.9

Total for Process - 3.27  $\frac{1980\$}{\text{Peak Watt}}$

cost represented by each step. Note that, in accordance with the JPL cost goals, the costs are determined using 1980 dollars.

The largest cost contribution comes from the first step: Preparation of input web. This step includes the cost of polycrystal silicon (\$14/kg), growth of the dendritic web, and cleaning operations required prior to diffusion of junctions.

Table 20 presents similar results for the fully automated 25 MW/yr production facility. Note here that almost 50% of the total cost is associated with the raw materials and growth of the dendritic web material. The other major cost driving step in the process is the module lamination step. The most significant portion of the cost of this step is the raw material cost for glass, EVA, and Mylar backing material.

Table 21 presents a breakdown of cost categories for the two production facilities. This is presented to show how the costs are driven by labor, materials, utilities, capital expenses, and taxes.

The simulation data indicates that extrapolation of the 1 MW/yr MEPSDU process to a 25 MW/yr production facility leads to a cost effective manufacturing sequence which essentially meets the DOE/JPL cost goals of 70¢/watt (1980 dollars) in 1986. The scaling was based on the assumption of a highly automated process, both within a given step and between process steps. This assumption reduces the labor content of the product cost. The material costs were scaled at a ratio of 19:1 usage factor for a 25:1 production ratio. Therefore, only minimal savings are assumed for material costs in the scale up.

TABLE 20

## SAMICS COST ANALYSIS

Value Added for Process Step

25 MW/yr Production Facility

<u>Process Step</u>	<u>Process</u>	<u>Value Added (1980\$/peak watt)</u>	<u>Percent of Total</u>
1	Prepare Input Web	0.340	49.5
2	Boron Diffusion	0.033	4.5
3	Phosphorous Diffusion	0.024	3.3
4	Application of AR/PR	0.016	2.2
5	Define Grid Pattern	0.017	2.4
6	Metallize Web	0.037	5.1
7	Rejection and Plating	0.046	6.3
8	Cell Separation and Test	0.029	4.0
9	Cell Interconnection	0.026	3.6
10	Lamination	0.121	16.6
11	Crating	0.019	2.5

Total for Process - 0.709  $\frac{1980\$}{\text{Peak Watt}}$

TABLE 21

## SAMICS COST ANALYSIS

Value Added per Watt Cost Factors for  
the 1 MW/yr and 25 MW/yr Simulations

(All Costs in 1980\$)

	<u>1 MW/yr</u>	<u>25 MW/yr</u>
Direct Labor	0.820	0.060
Direct Materials	0.539	0.388
Direct Utilities	0.033	0.008
Indirect Labor	0.469	0.038
Indirect Materials	0.060	0.004
Indirect Utilities	0.044	0.005
Capital Expenses	0.770	0.111
Taxes/Misc.	0.521	0.095

IX. DOCUMENTATION

All contractual documentation requirements associated with the MEPSDU contract were met during the course of the program. These documents and their submittal dates are summarized in Table 22.

TABLE 22  
MEPSDU PROGRAMMABLE DOCUMENTATION SUBMITTAL STATUS

<u>ITEM</u>	<u>SUBMITTAL DATE(S)</u>
1. COST ESTIMATES	
a. Baseline	December 17, 1980
b. Revision 1	May 22, 1981
c. Revision 2	January 8, 1982
2. SCHEDULE ACCOMPLISHMENT REPORT/FINANCIAL REPORT	December 17, 1980 January 14, 1981 February 16, 1981 March 16, 1981 April 16, 1981 May 16, 1981 June 16, 1981 July 16, 1981 August 17, 1981 October 15, 1981 November 16, 1981 January 15, 1982 February 16, 1982
3. PROGRAM PLAN AND WBS	
a. Original	December 17, 1980
b. Revision 1	May 22, 1981
c. Revision 2	January 8, 1982
4. MONTHLY TECHNICAL PROGRESS REPORT	January 15, 1981 February 15, 1981 March 15, 1981 April 15, 1981 May 15, 1981 June 4, 1981 July 6, 1981 August 6, 1981 September 8, 1981 October 8, 1981 November 5, 1981 December 11, 1981 January 12, 1982
5. PRELIMINARY DESIGN REVIEW PACKAGE	February 19, 1981
6. MODULE DESIGN REVIEW PACKAGE	June 30, 1981
7. QUARTERLY TECHNICAL PROGRESS REPORT	March 15, 1981 June 15, 1981 September 15, 1981 December 15, 1981